THE GOTHIC SHALE OF THE PENNSYLVANIAN PARADOX FORMATION, GREATER ANETH FIELD (ANETH UNIT), SOUTHEASTERN UTAH: SEAL FOR HYDROCARBONS AND CARBON DIOXIDE

by Jason E. Heath, Thomas A. Dewers, Thomas C. Chidsey, Jr., Stephanie M. Carney, and S. Robert Bereskin

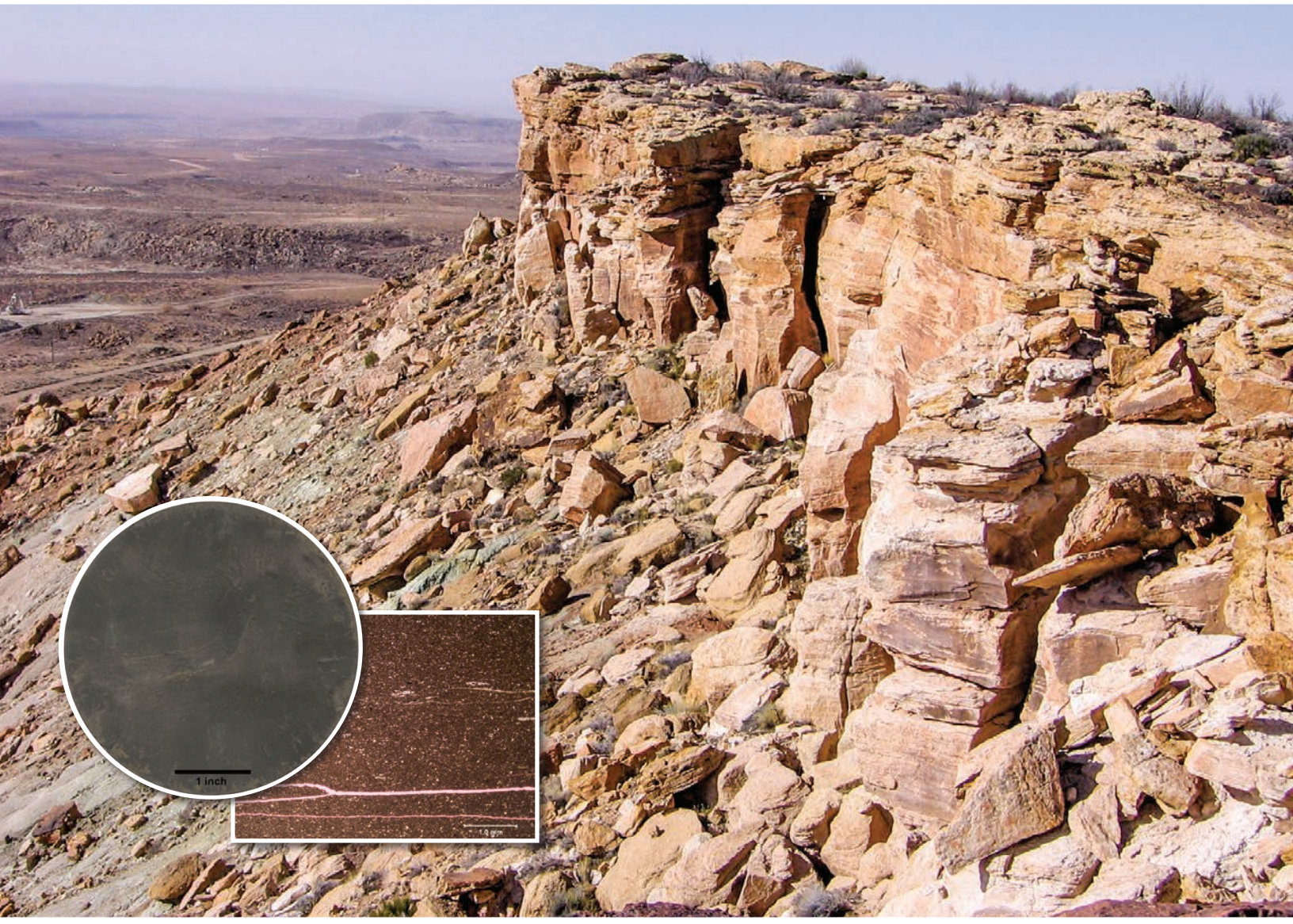

MISCELLANEOUS PUBLICATION 17-1
UTAH GEOLOGICAL SURVEY
a division of
UTAH DEPARTMENT OF NATURAL RESOURCES
2017

Blank pages are intentional for printing purposes

THE GOTHIC SHALE OF THE PENNSYLVANIAN PARADOX FORMATION, GREATER ANETH FIELD (ANETH UNIT), SOUTHEASTERN UTAH: SEAL FOR HYDROCARBONS AND CARBON DIOXIDE

by Jason E. Heath[1], Thomas A. Dewers[1], Thomas C. Chidsey, Jr.[2], Stephanie M. Carney[2], and S. Robert Bereskin[3]

[1]Sandia National Laboratories, Albuquerque, New Mexico
[2]Utah Geological Survey, Salt Lake City, Utah
[3]Bereskin and Associates, Salt Lake City, Utah

Cover photos: Cross-bedded channel deposits of the Cretaceous Dakota Formation overlying varigated shales of the Brushy Basin Member of the Jurassic Morrison Formation, Aneth Unit (view west), Greater Aneth field, southeastern Utah. Photo by Craig D. Morgan, Utah Geological Survey. Left inset: typical Gothic shale core (view down core) of the Pennsylvanian Paradox Formation, which forms the reservoir seal for Greater Aneth field. Right inset: photomicrograph (plane light) of argillaceous shale lithotype in the Gothic shale. Both images from 5379.4 feet (1639.6 m), Aneth Unit No. H-117 well.

ISBN: 978-1-55791-940-3

MISCELLANEOUS PUBLICATION 17-1
UTAH GEOLOGICAL SURVEY
a division of
UTAH DEPARTMENT OF NATURAL RESOURCES
2017

STATE OF UTAH
Gary R. Herbert, Governor

DEPARTMENT OF NATURAL RESOURCES
Michael Styler, Executive Director

UTAH GEOLOGICAL SURVEY
Richard G. Allis, Director

PUBLICATIONS
contact
Natural Resources Map & Bookstore
1594 W. North Temple
Salt Lake City, UT 84116
telephone: 801-537-3320
toll-free: 1-888-UTAH MAP
website: mapstore.utah.gov
email: geostore@utah.gov

UTAH GEOLOGICAL SURVEY
contact
1594 W. North Temple, Suite 3110
Salt Lake City, UT 84116
telephone: 801-537-3300
website: geology.utah.gov

CONTENTS

FIGURES

TABLES

THE GOTHIC SHALE OF THE PENNSYLVANIAN PARADOX FORMATION, GREATER ANETH FIELD (ANETH UNIT), SOUTHEASTERN UTAH: SEAL FOR HYDROCARBONS AND CARBON DIOXIDE

by Jason E. Heath, Thomas A. Dewers, Thomas C. Chidsey, Jr., Stephanie M. Carney, and S. Robert Bereskin

ABSTRACT

Greater Aneth oil field, Utah's largest oil producer, was discovered in 1956 and has produced over 483 million barrels of oil. Located in the Paradox Basin of southeastern Utah, Greater Aneth is a stratigraphic trap producing from the Pennsylvanian (Desmoinesian) Paradox Formation. Because Greater Aneth is a mature, major oil field in the western U.S., and has a large carbonate reservoir, it was selected to demonstrate combined enhanced oil recovery and carbon dioxide storage. The Aneth Unit in the northwestern part of the field has produced over 160 million barrels of the estimated 386 million barrels of original oil in place—a 42% recovery rate. The large amount of remaining oil made the Aneth Unit ideal to enhance oil recovery by carbon dioxide flooding and demonstrate carbon dioxide storage capacity.

Within the Paradox Formation, the Gothic shale seals the underlying Desert Creek oil reservoir. The Gothic shale ranges in thickness from 7 to 26 feet (2–8 m), averaging 15 feet (4.6 m). Within the Aneth Unit, it is remarkably uniform consisting of black to gray, laminated to thin-bedded, dolomitic marine shale. The Gothic contains total organic carbon ranging from 2.2% to 4.4% with type III and mixed type II-III kerogen. Natural fractures are horizontal to inclined (30° to 44°) with evidence of shear in the form of slickensides; some mineralization is present. Geochemical, petrological, petrophysical, and geomechanical analyses were conducted to determine (1) the geologic controls on sealing effeciency, (2) effects of pressure changes on the seal due to carbon dioxide injection and storage, and (3) possible chemical interaction between carbon dioxide and the seal at its contact with the reservoir through time.

INTRODUCTION

Greater Aneth oil field, Utah's largest oil producer, was discovered in 1956 and has produced over 483 million barrels of oil (BO) (Utah Division of Oil, Gas and Mining, 2017a). It is a mature, major oil field in the western U.S. and has a large carbonate reservoir. Located in the Paradox Basin of extreme southeastern Utah (figure 1) within the Colorado Plateau, Greater Aneth is a stratigraphic trap created by facies changes that seal the reservoir laterally in addition to the seals above and below; fractures and small faults create a structural component to the field. Greater Aneth produces oil and gas from the Desert Creek zone of the Pennsylvanian (Desmoinesian) Paradox Formation (figure 2). The Desert Creek zone is a complex reservoir representing a variety of depositional environments (open-marine shelf, shallow-marine oolitic shoals, phylloid-algal mounds, low-energy restricted shelf) that produce significant heterogeneity. There is some evidence of minor hydrothermal dolomite, in-situ brecciation, and faults that may affect fluid flow (Chidsey and Eby, 2014). Original oil in place (OOIP) reserves for Greater Aneth field are estimated at 1100 million barrels (bbls) (Babcock, 1978a, 1978b, 1978c, 1978d; Peterson, 1992). Thus, given the large amount of remaining oil, the field was ideal for enhanced oil recovery (EOR) by carbon dioxide (CO_2) flooding and a demonstration of CO_2 storage capacity.

Paradox Formation shale, halite, and anhydrite at Greater Aneth field serve as vertical reservoir seals. Lateral seals are permeability barriers created by unfractured, off-mound (non-buildup) mudstone and wackestone. The Gothic shale of the Paradox Formation separates the Ismay from the underlying Desert Creek zones in Greater Aneth (figure 2) and other fields in the basin. It is the primary seal for the Des-

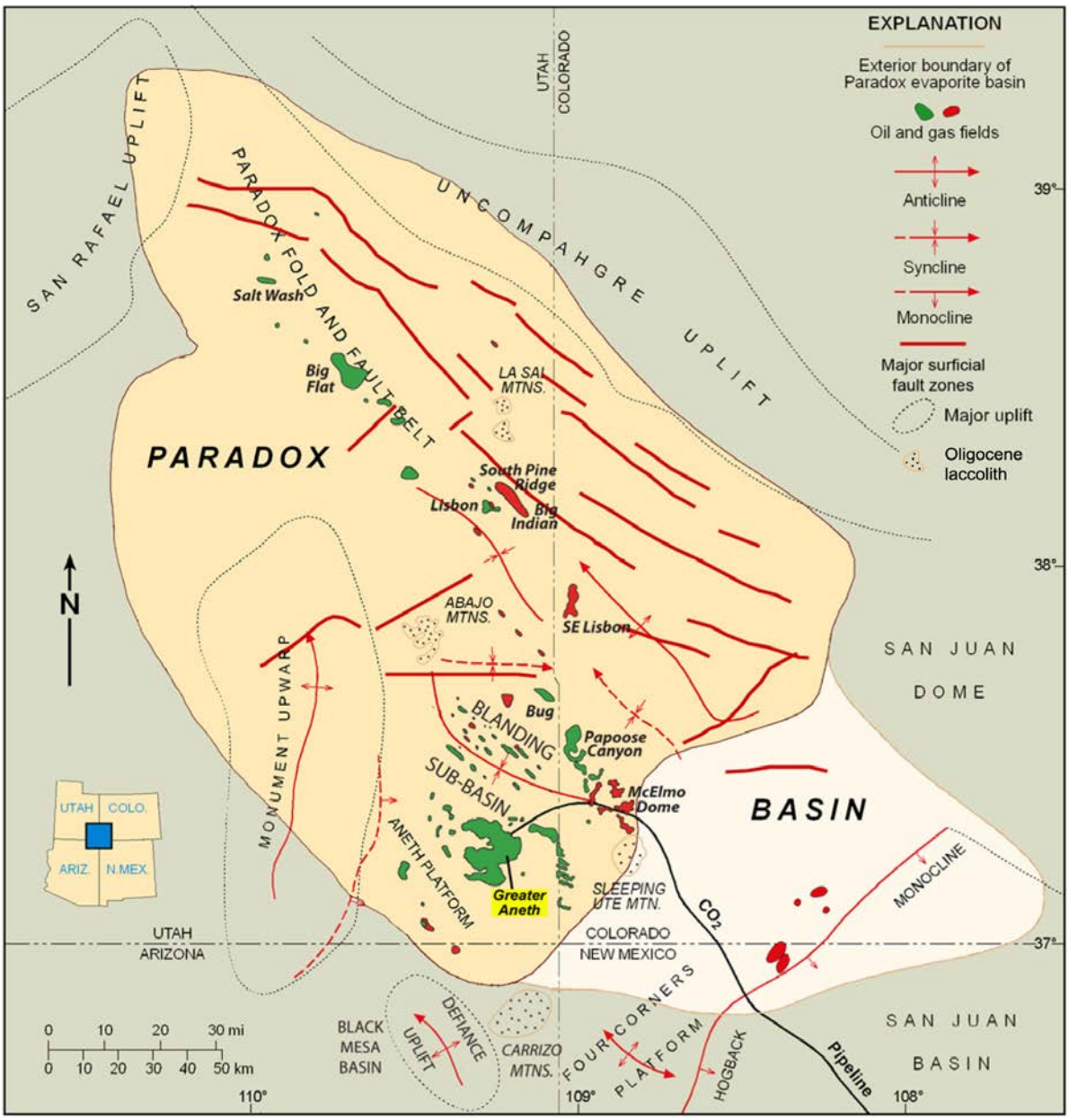

Figure 1. *Oil and gas fields in the Paradox Basin of Utah, Colorado, and Arizona. The Paradox Formation play is shaded light orange. Note location of Greater Aneth field in southeasternmost Utah. Modified from Kitcho (1981) and Harr (1996).*

ert Creek reservoir, although the Gothic is now recognized as a potential shale-gas or shale-oil reservoir in this area of the Paradox Basin (Schamel, 2005, 2006; Bereskin and McLennan, 2008, 2009; Bereskin and others, 2010; Chidsey, 2016). The Gothic shale is widespread throughout the Paradox Basin, but is only exposed in Utah along parts of the San Juan River west of the Aneth area (Morgan and others, 2016). In the Aneth Unit, the Gothic shale is remarkably uniform, consisting of black to gray, laminated to thin-bedded, organic-rich dolomitic marine shale. It averages 15 feet (4.6 m) thick and generally thins over the carbonate buildup complex in the Desert Creek zone.

A reservoir seal can be defined as a body of rock that is capable of significantly impeding the migration or movement of oil, natural hydrocarbon gas, and CO_2 (Couples, 2005). Diffusion in this case is not considered an important means for moving hydrocarbons or CO_2. Key relationships to consider in understanding seals include those between porosity and (1) stress, (2) permeability, and (3) capillary breakthrough pressure (Alpin and Larter, 2005). These relationships are affected by the seal's petrographic (grain size, mineral composition, and clay fraction) and geochemical (organic content and maturity) characteristics. The ability of mudrock (shale), salt, and anhydrite to prevent CO_2 (and hydrocarbon) leakage is a critical factor for the geological storage of anthropogenic CO_2 (Lu and others, 2009). For effective storage of CO_2 produced from coal-fired power plant point sources, retention times of 10,000 years are required (Lindeberg, 2002). Therefore, it is critical to under-

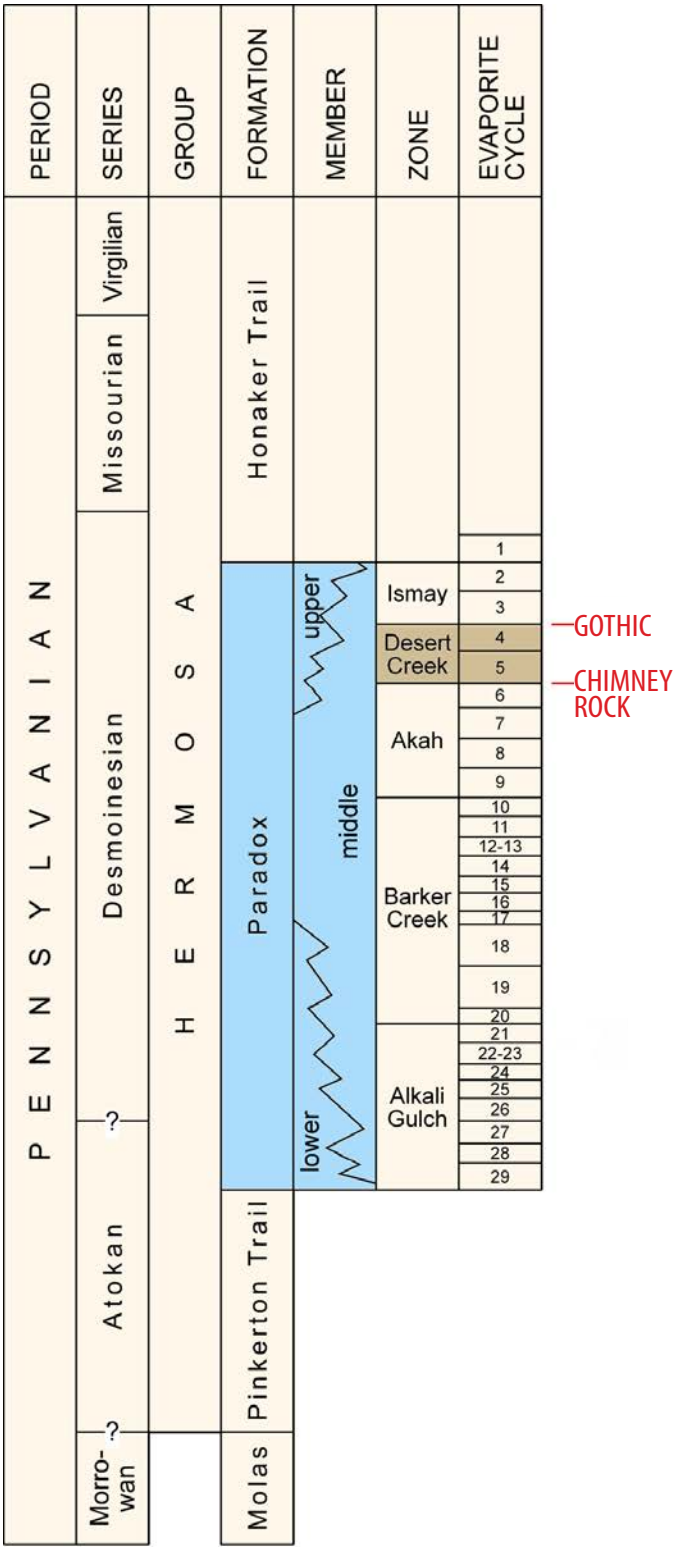

Figure 2. *Pennsylvanian stratigraphic chart for the Paradox Basin including the Paradox Formation, informal zones (Desert Creek in tan), and numbered cycles. Red text points to the organic-rich Gothic and Chimney Rock shale intervals that serve as both hydrocarbon source and seals for the Desert Creek zone at Greater Aneth field. Modified from Hite (1960), Hite and Cater (1972), and Reid and Berghorn (1981).*

stand if the seal can remain effective for long periods of time (Lu and others, 2009). For large-scale geologic CO_2 storage, additional questions not part of a typical hydrocarbon reservoir seal analysis must be addressed. These include:

1. Can the impact of preexisting seal fractures on CO_2 transport be adequately characterized prior to CO_2 injection?
2. What chemical alterations of seal rock minerals and/or organic matter would occur from interaction with CO_2-rich fluids, and how would they affect sealing capacity?
3. What rate and amount of CO_2 leakage would be acceptable?
4. What geomechanical impacts, such as fracture creation or containment problems, accompany CO_2 injection?

A major challenge is identifying local micro- to meso-scale imperfections or flaws in seals that could allow CO_2 to migrate from potential storage sites, which may cover areas up to hundreds of square miles. We investigated these questions at Greater Aneth field, as part of a demonstration study by the Southwest Regional Partnership on Carbon Sequestration conducted from 2006 through 2010, to develop and test conceptual and numerical models of sealing behavior with a focus on understanding pre-existing natural imperfections and the potential formation of new imperfections.

The following activities were conducted on the Gothic shale: (1) subsurface mapping, (2) general core description, (3) geochemistry, (4) petrography, (5) analysis of natural fractures, (6) petrophysical properties, and (7) geomechanics. The study results were used to determine the geologic controls on seal efficiency, effects of pressure changes on seal efficiency due to CO_2 injection and storage, and chemical interaction between CO_2 and the seal at its contact with the reservoir through time.

GREATER ANETH FIELD SYNOPSIS

Greater Aneth field is divided into four drilling units (figure 3). The 25-square-mile (65 km^2) Aneth Unit (T. 40 S., R. 23 to 24 E., Salt Lake Base Line and Meridian, San Juan County) is located in the northwestern part of the field. The majority of the unit is located on Navajo Nation lands, with the exception of the western part, which is U.S. Bureau of Land Management (BLM) parcels.

Trap and Lithofacies

The Greater Aneth field stratigraphic trap produces primarily from the Desert Creek zone, which is sealed and sourced by the organic-rich, overlying Gothic and underlying Chimney Rock

shales, respectively (figure 2). The Desert Creek zone creates an irregular west-northwest-trending reservoir buildup (figure 4). The trap was created by facies changes, including evaporites, that seal the reservoir laterally in addition to the seals above and below. Within the field, the Desert Creek zone is divided into three subzones: a relatively thin lower interval that represents a transition to the Chimney Rock shale, a middle interval composed predominantly of phylloid-algal buildup lithofacies, and an upper interval composed of oolitic-peloidal calcarenite lithofacies (Peterson and Ohlen, 1963; Babcock, 1978a, 1978b, 1978c, 1978d; Peterson, 1992; Moore and Hawks, 1993; Chidsey and Eby, 2014). The Desert Creek reservoir at Greater Aneth field consists of limestone (algal bafflestone and oolitic, peloidal, and skeletal grainstone and packstone) and finely crystalline dolomite.

The depositional environment for the Gothic shale was generally low-energy, offshore marine based on a limited number of cores from wells in the Utah part of the Paradox Basin (for detailed core descriptions and core photographs see Chidsey, 2016). Anaerobic, dysaerobic, or anoxic conditions existed in deep water settings. Slow deposition also included some clastic influx from a distal source consisting of dysaerobic, organic-rich material diluted by terrigenous clastic sediments. Water depths were probably variable, ranging from below fair-weather and storm wave base for the organic-rich shales to relatively shallow, nearshore for siltier intervals. Influx of terrigenous quartz silt in the Gothic associated with the Silverton delta in the easternmost Paradox Basin in southwestern Colorado, combined with organic-rich material, helped create reservoirs with some marginal shale-gas production in that part of the basin (Moreland and Wray, 2009). The source of the quartz silt in the Gothic within the Utah part of the Paradox Basin was probably to the west-southwest.

Reservoir Properties

The average net reservoir thickness of the Desert Creek zone at Greater Aneth is 50 feet (15 m) over a 48,260-acre (19,530 ha) area. Porosity ranges from 9% to 13% (but can be significantly higher, 16% or greater) in interparticle, moldic, and intercrystalline networks enhanced by fractures; permeability averages 10 millidarcies (mD), ranging from 3 to 100s mD. The original drive mechanism is fluid expansion and solution gas; original water saturation was 24%. The bottom-hole temperature averages 125°F (52°C) (Peterson and Ohlen, 1963; Babcock, 1978a, 1978b, 1978c, 1978d; Peterson, 1992; Moore and Hawks, 1993).

Hydrocarbon Characteristics

The produced oil is a dark green, paraffinic crude. The oil was originally sweet but now is sour due to sulfate-reducing bacteria introduced during waterflood operations. The API gravity of the oil ranges from 40° to 42°; the original gas-oil ratio was 665 cubic feet/bbl. The viscosity of Greater Aneth oils ranges 0.53 to 0.54 centipoise. The pour point of the crude oil is 10°F (-12°C). The average weight percent sulfur and nitrogen of produced hydrocarbon liquids are 0.2 and 0.04, respectively (Stowe, 1972; Peterson, 1992). Greater Aneth reservoirs produce associated gas that is fairly uniform in composition, averaging 62% methane, 18% ethane, 11% propane, 5.5% butane and iso-butane, 2.5% pentane and iso-pentane, less than 1% hexane and higher fractions, 0.2% CO_2, and occasionally a trace of hydrogen sulfide and helium (Stowe, 1972; Moore and Hawks, 1993). The gas heating value averages 1450 British thermal units/cubic foot (Btu/ft^3) (1.53 million joules). The to-

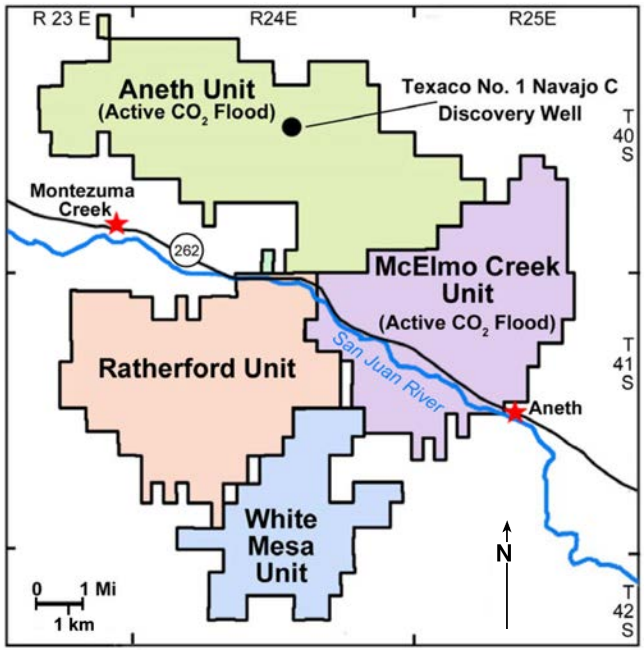

Figure 3. *Drilling units within Greater Aneth field, San Juan County, Utah.*

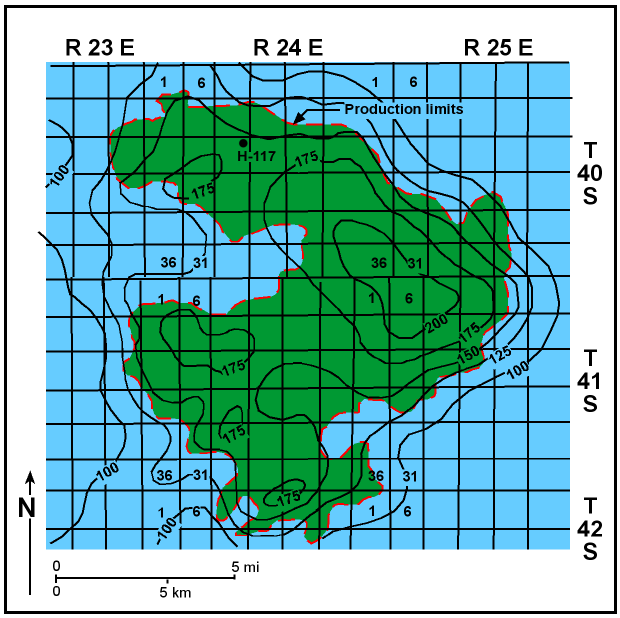

Figure 4. *Generalized isopach of the Desert Creek zone, Greater Aneth field, San Juan County, Utah; contour interval = 25 feet. Note the location of the Aneth Unit No. H-117 well (NE1/4NE1/4 section 17, T. 40 S., R. 24 E., Salt Lake Base Line & Meridian). Modified from Peterson and Ohlen (1963).*

tal dissolved solids in the produced water ranges from 103,000 to 304,000 mg/L; the resistivity of the water is 0.35 ohm-meters at formation temperature (Peterson, 1992).

Production, Reserves, and Enhanced Oil Recovery

Greater Aneth field was discovered in February 1956 with the completion of the Texaco No. 1 Navajo C well, NW1/4NE1/4 section 23, T. 40 S., R. 24 E. (figure 3), which had an initial flowing potential (IFP) of 568 bbls of oil per day (BOPD) and 4376 thousand cubic feet of gas per day (MCFGPD). The original reservoir field pressure was 2170 pounds per square inch (psi [14,960 kPa]) (Moore and Hawks, 1993). Currently, 444 producing (or shut-in) wells and 123 abandoned producers are in the field. Cumulative production as of January 1, 2017, was 483.1 million BO, 440.2 billion cubic feet of gas (BCFG), and 1879.5 million bbls of water (BW) (Utah Division of Oil, Gas and Mining, 2017a). The OOIP reserves for Greater Aneth field are estimated at 1100 million bbls (Babcock, 1978a, 1978b, 1978c, 1978d; Peterson, 1992).

Waterflood operations began in 1961 and are used in all four Greater Aneth field units (figure 3)—the largest waterflood program in Utah (Babcock, 1978b). More than 340 water injection wells exist in the field in 2016 (over 500 injection wells in the past) (Utah Division of Oil, Gas and Mining oil and gas database). Both fresh and produced water are used. The EOR waterflood programs at Greater Aneth field units using vertical wells will ultimately recover 8% to 30% of the OOIP or approximately 230 million BO (37 million m^3), whereas primary recovery was about 200 million BO or 15% to 25% of the OOIP (Babcock, 1978a, 1978b, 1978c, 1978d; Peterson, 1992).

Carbon dioxide flooding, through a water-alternating-gas (WAG) program, began in the McElmo Creek Unit in 1985 (figure 3). Production increased in unit wells between one and two years. The Devonian Ouray Formation and Mississippian Leadville Limestone, at McElmo Dome field on the eastern edge of the Paradox Basin in southwest Colorado, supply CO_2 to Greater Aneth field (and Permian Basin fields) via an 8-inch pipeline (figure 1). A pilot CO_2 flood using horizontal wells (lateral) was conducted in the eastern part of the Aneth Unit in 1998.

Extensive and successful horizontal drilling programs have been conducted in Greater Aneth field. These drilling programs were carried out primarily in the Aneth (in 1996) and Ratherford (in 1994) Units in the northwest and southeast parts of the field, respectively (figure 3). Northwest-southeast-directed horizontal wells in the Desert Creek zone, perpendicular to the fault/fracture zones, have successfully increased production in these units (Amateis, 1995).

Production in the Aneth Unit had declined by 50% over the past 20 years as the waterflood operations and horizontally drilled wells have matured. Primary recovery was 58.4 million BO (15%) and secondary recovery from waterflooding was 76.7 million BO (20%), respectively, of the estimated 386 million bbls of OOIP (Babcock, 1978a). However, production has improved due to a CO_2 flood program initiated in 2007 by the current field operator, Resolute Energy Corporation. Incremental recovery from CO_2 flooding is estimated at 33 million BO or an additional incremental recovery efficiency of 9% (Jim Rutledge, Los Alamos National Laboratory, verbal communication, 2007). The Aneth Unit has produced over 160 million BO as of January 1, 2017 (Utah Division of Oil, Gas and Mining, 2017b)—a 42% recovery rate.

THE GOTHIC SHALE IN THE ANETH UNIT

Subsurface Structural and Thickness Mapping

The Gothic shale is the seal for the Desert Creek oil reservoir and injected CO_2 in the Aneth Unit. The structure contour and thickness maps for the Gothic are shown on figures 5 and 6, respectively. The lateral extent and shape of the underlying Desert Creek carbonate buildup complex is seen in the structure contour map as elevated areas within the Aneth Unit. Structural mapping of the Gothic also suggests the presence of faults that are undetected on seismic data or on wireline well logs, but are expressed only as unusual or localized shifts in contour orientation. Most notably are possible northeast-southwest trending faults in the southwest corner of section 18, T. 40 S., R. 24 E., and in section 29, T. 40 S., R. 25 E. (figure 5). Hydrothermal (saddle) dolomite, intense brecciation, doubly terminated quartz, and other evidence of faulting are present in core from the Desert Creek zone in the Aneth Unit No. E-418 well (NW1/4SW1/4SW1/4 section 18, T. 40 S., R. 24 E.) (Chidsey and Eby, 2014). However, the northeast-southwest strike of these potential faults as seen on the structure contour map do not match the known structural northwest-southeast trend of other, deeper faults in the area. For example, three-dimensional (3-D) seismic specifically of Greater Aneth field shows basement faults of Mississippian and Pennsylvanian age that strike northwest-southeast (Mike Tryggestad, formerly with Resolute Natural Resources, verbal communication, 2009). Also, the unusual northeast-striking faults do not appear in structure contour maps of overlying strata such as the DeChelly and Navajo Sandstones, and therefore, are likely localized structures with minimal displacement. The postulated fault near the Aneth Unit No. E-418 well could be a potential migration pathway for CO_2 between the Ismay and Desert Creek reservoirs, but since the fault does not appear to extend outside of the Paradox Formation, the risk of leakage into overlying strata is small.

The Gothic shale within the Aneth Unit ranges from 7 to 26 feet (2–8 m) thick and thins to the southeast (figure 6), indicating slightly shallower water to the southeast during the time of deposition; regional mapping of the Gothic shows thicknesses ranging from 2 to 70 feet (0.6–21 m) (Chidsey, 2016). An area of very thin shale (4 to 6 feet [1.2–1.8 m]) occurs in section 23, T. 40 S., R. 24 E., which is coincident with a thickened interval in the Desert Creek zone. This indicates that the shale was likely deposited on a high-relief carbonate buildup. We be-

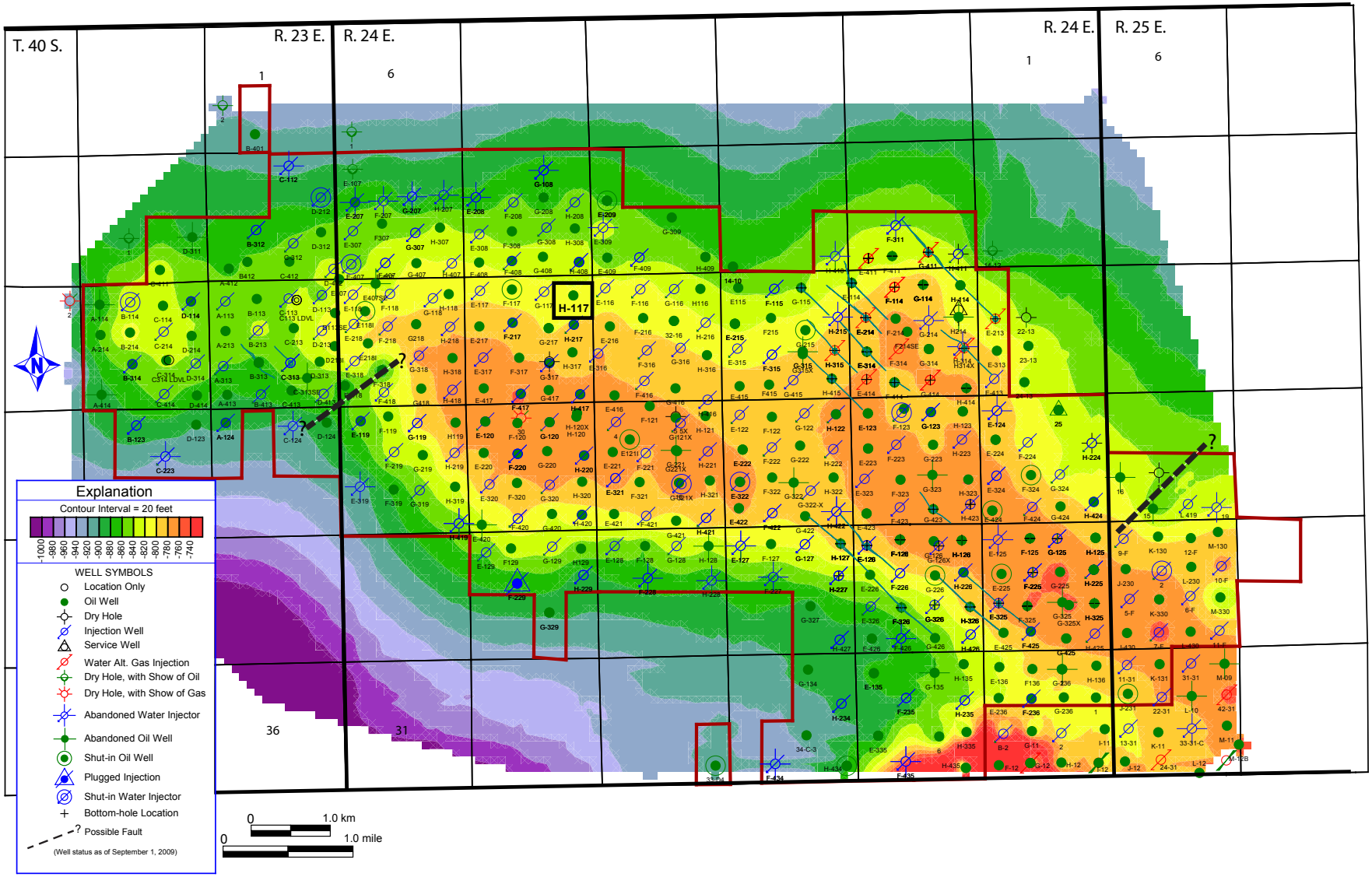

Figure 5. *Structure contours on the top of the Gothic shale, Aneth Unit, Greater Aneth field. Aneth Unit shown by red outline; note the location of the Aneth Unit No. H-117 well (black box in NE1/4NE1/4 section 17, T. 40 S., R. 24 E.).*

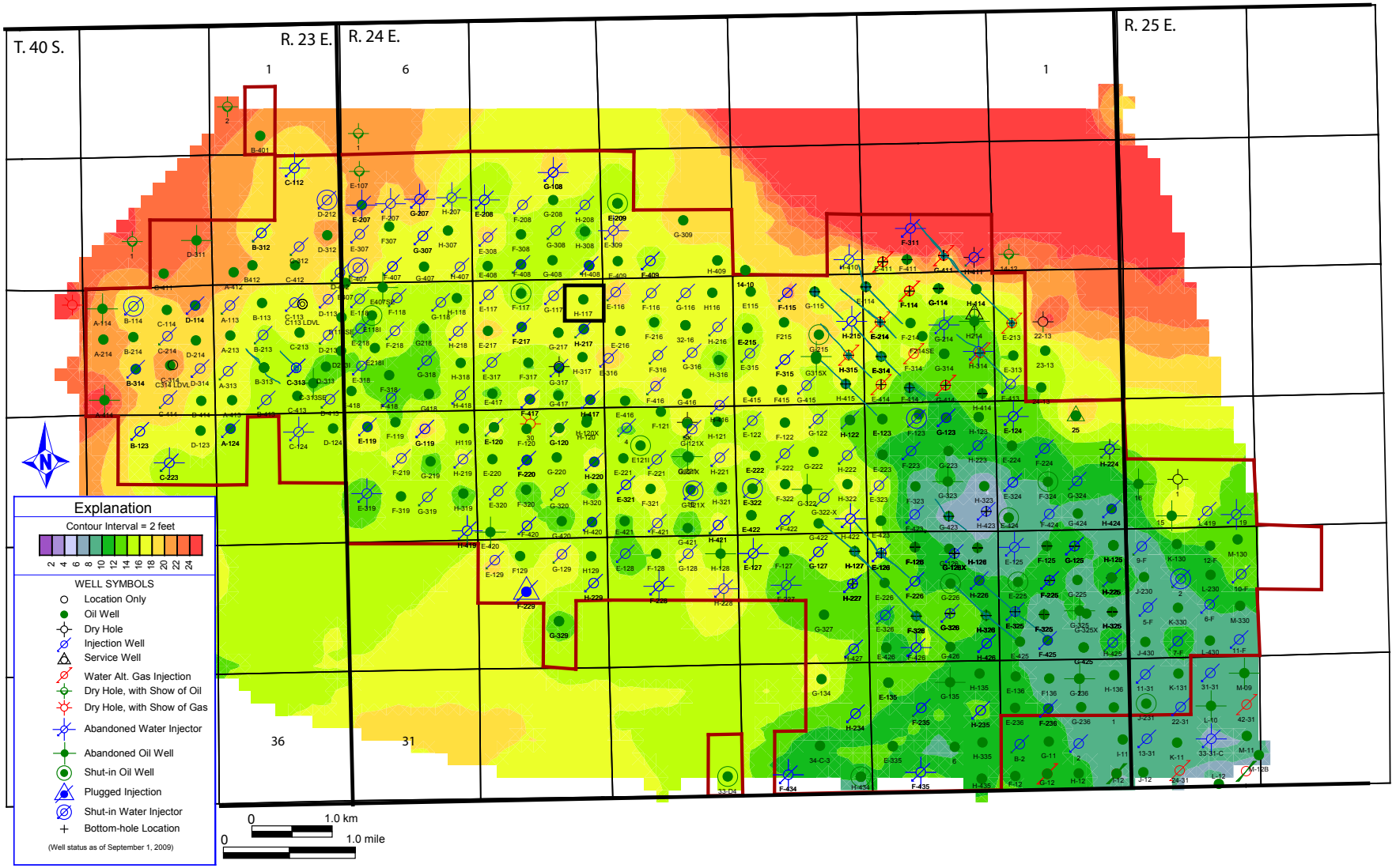

Figure 6. *Thickness of the Gothic shale, Aneth Unit, Greater Aneth field. Aneth Unit shown by red outline; note the location of the Aneth Unit No. H-117 well (black box in NE1/4NE1/4 section 17, T. 40 S., R. 24 E.).*

lieve that the integrity of the seal of the Desert Creek is unaffected by this area of thin Gothic shale. The two wells located in SE1/4 section 23 penetrated the thinnest section of Gothic but have produced 226,505 BO and 1,023,549 BO from the Desert Creek, respectively (Utah Division of Oil, Gas and Mining, 2017b), implying the presence of a high-quality seal. In addition, much of the overlying lower Ismay and uppermost Desert Creek zones throughout the Aneth Unit are non-reservoir rock (widespread low-permeability carbonates and siltstones) and provide secondary seals, as do anhydrite intervals common laterally in the upper Desert Creek itself away from the productive limits of Greater Aneth field (Peterson, 1992; Chidsey and others, 1996; Chidsey and Eby, 2014).

General Core Description

When most of the development drilling of Greater Aneth field occurred during the 1950s and 1960s, the goal of coring operations was to acquire core from the Desert Creek reservoir, not the overlying Gothic shale. However, core from the Aneth Unit No. H-117 well (SW1/4NE1/4NE1/4 section 17, T. 40 S., R. 24 E., figure 4) contains nearly a complete (16 feet [4.9 m]), unslabbed section of Gothic shale (figures 7 and 8); this core and other Greater Aneth cores are publicly available at the Utah Core Research Center (UCRC) in Salt Lake City, Utah. This core is ideal for detailed representative analysis of the Gothic seal for the Desert Creek reservoir in the Aneth Unit. Comprehensive geological description of core is essential to define lithologic units and, in combination with petrological analysis, provides the fundamental mineralogical, textural, and diagenetic factors defining the seal. In the Gothic shale, seemingly subtle variations in mineralogical character, cementation, or depositional environment result in important changes in seal capacity or result in mechanical boundaries. These subtle differences in turn control fracture spacing, distribution, orientation, and conductivity.

The Gothic shale strata consist of a fairly monotonous interval of dark brown to dark gray, faintly wavy laminated, calcareous mudstone (figure 8B). Variable amounts of terrigenous quartz, chert, feldspar, micas, illitic and chloritic clays, phosphate, some carbonaceous material, and fossil fragments are present in this core. Both megafossils and microfossils are present (transported and indigenous) including calcareous bivalve mollusks and ostracods, inarticulate brachiopods, phosphatic conulariids, conodonts, arenaceous foraminifera, and possible spores of indeterminate origin. Diagenetic products include abundant pyrite and varying amounts of rare to common dolomite/ankerite. Modest amounts of clay microporosity likely exists, but the permeability is in the nannodarcy range.

The basal portion of the Gothic shale appears to be the most organic rich, containing a total organic content (TOC) of 4.4%, whereas the section above contains less than 3% TOC (table 1). Here a flooding event transgressed over older mottled carbonates with possible subaerial pisolitic character. In some instances, the basal mudstone appears to have eroded the underlying limestones, depositing a basal lag rich in bivalve mollusks. Above this basal lag, the lower portion of the Gothic contains a wider assemblage of phosphatic con-

Figure 7. *Core (unslabbed) of the Gothic shale from the Aneth Unit No. H-117 well. Scale bars = 2 feet (showing tenths of a foot increments).*

stituents—conodonts, conulariids, and indistinct (fish) fragments, as well as pyrite throughout the section.

Most of the depositional environments for the Gothic shale in the Aneth Unit No. H-117 core were the same low-energy, offshore marine typically described elsewhere in the Paradox Basin. Deep-water conditions were dysaerobic to anoxic. The quartz silt in some intervals also represents the clastic influx redeposited from the source to the west-southwest observed elsewhere in the Paradox Basin of Utah, where or when water depths were shallower and the shoreline closer.

Only two other Aneth Unit cores currently stored at the UCRC penetrated part of the Gothic shale—the Aneth Unit No. E-418 well (NW1/4SW1/4SW1/4 section 18, T. 40 S., R. 24 E.) and Aneth Unit No. 27-C-3 well (NW1/4SE1/4 section 18, T. 40 S., R. 24 E.). These wells are located 2 miles (3.2 km) west-southwest and 3.5 miles (5.6 km) southeast, respectively, from the Aneth Unit No. H-117 well. The cores were examined for this study (for detailed core descriptions and core photographs see Chidsey and Eby, 2014) and show little lateral lithologic variability in the Gothic from what was observed in the Aneth Unit No. H-117 core.

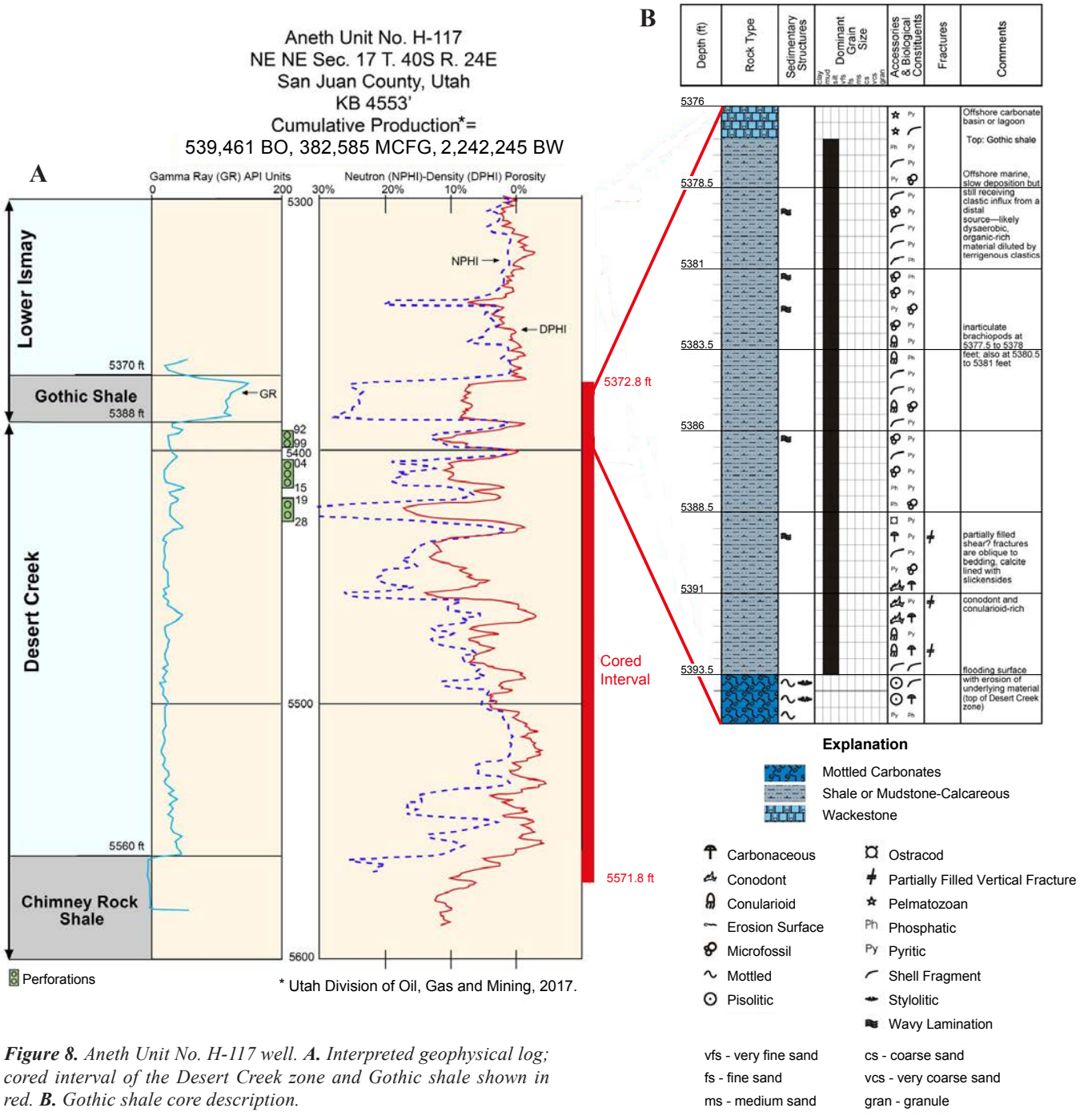

Figure 8. *Aneth Unit No. H-117 well.* ***A.*** *Interpreted geophysical log; cored interval of the Desert Creek zone and Gothic shale shown in red.* ***B.*** *Gothic shale core description.*

Table 1. *Basic geochemical measurements from the Gothic shale in the Aneth Unit No. H-117 well.*

Depth (ft)	As-Received Bulk Density (g/cc)	TOC[1]	S1[2]	S2[3]	S3[4]	T_{max}[5]	HI[6]	OI[7]	S2/TOC	PI[8]	Calc R_o[9]
5379.40	2.570	2.89	2.09	6.45	0.73	445	224	25	72	0.24	0.85
5382.80	2.561	2.81	2.16	5.97	0.64	451	213	23	77	0.27	0.96
5386.90	2.572	2.23	1.93	5.15	0.84	444	231	38	87	0.27	0.83
5390.80	2.522	4.42	2.39	9.46	0.76	449	214	17	54	0.20	0.92

[1]TOC = total organic carbon (wt.%)
[2]S1 = amount of free hydrocarbons in the sample (mg HC/g rock)
[3]S2 = amount of hydrocarbons generated by pyrolytic degradation of kerogen (mg HC/g rock)
[4]S3 = amount of CO_2 (mg CO_2/g rock) produced during pyrolysis of kerogen
[5]T_{max} = temperature (ºC) of maximum release of hydrocarbons from cracking of kerogen during pyrolysis
[6]HI = hydrogen index, the ratio of the amount of hydrogen relative to the amount of organic carbon present in a sample; (S2/TOC) x 100
[7]OI = oxygen index, the ratio of the amount of oxygen relative to the amount of organic carbon present in a sample; (S3/TOC) x 100
[8]PI = production index, the ratio of already generated hydrocarbons to potential hydrocarbons; S1/(S1 + S2)
[9]Calc R_o = calculated vitrinite reflectance (%)

Geochemistry

In the Colorado part of the Paradox Basin, the Gothic shale produces hydrocarbon shale gas. To understand the Gothic's effectiveness as a seal, a full understanding of any hydrocarbon potential as well as the long-term reactivity of organic content with CO_2 is required. Meaningful estimates of shale gas-in-place reserves—and subsequent deliverability of this gas—require accurate formation evaluation. These data are obtained by measuring the volume and rate of gas released by laboratory isotherm adsorption measurements. Lost gas analysis is then made to estimate original gas-in-place. Gas analysis and geochemical characterization provide fundamental complementary information for gas composition, organic content, kerogen type, and kerogen maturity. The following tests were conducted on the Aneth Unit No. H-117 core: (1) programmed pyrolysis (Rock-Eval™), (2) total organic component analysis, (3) calculated vitrinite reflectance, and (4) adsorption isotherms (tables 1 and 2).

In the Aneth Unit No. H-117 core, the Gothic shale has a TOC between 2.2% and 4.4%. The content of free hydrocarbons (gas and oil, S1) in the Gothic ranges from 1.9 to 2.4 mg/g, and the amount of hydrocarbons generated through thermal cracking of nonvolatile organic matter (S2) ranges from 5.2 to 9.5 mg/g. The amount of CO_2 (in milligrams CO_2 per gram of rock) produced during pyrolysis of kerogen (S3) ranges from 0.6 to 0.8 mg/g, and has important implications for geologic storage of CO_2 in the underlying Desert Creek zone, briefly discussed later. Kerogen type determination from TOC and programmed pyrolysis data shows the Gothic contains type II and mixed type II-III kerogen (figure 9), whereas kerogen quality analysis suggests it is gas prone (figure 10). Types II and III will generate oil and gas, respectively. Isotherm methane adsorption and Langmuir measurements (table 2 and figure 11) show gas versus pressure to evaluate adsorbed and interstitial gas content. Gas content

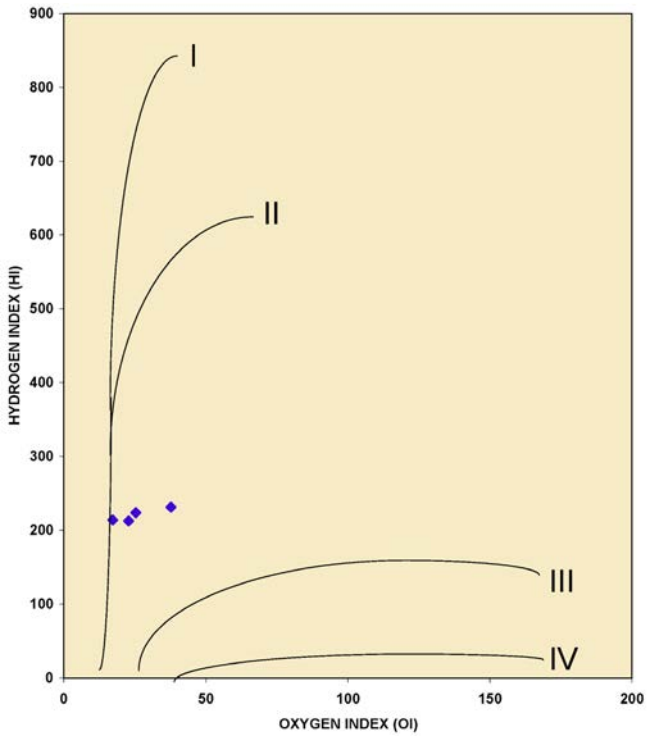

Figure 9. *Kerogen type determination of the Gothic shale from TOC and programmed pyrolysis data. The data indicate the Gothic contains type II and mixed type II/III kerogen. The hydrogen index (HI) represents the amount of hydrogen relative to the amount of organic carbon present in a sample. It is a ratio determined by the formula: HI = (S2/TOC) x 100, where S2 is the amount of hydrocarbons (HC) generated by the pyrolytic degradation of kerogen (mg HC/g rock) and TOC is the total organic carbon, in grams. The oxygen index (OI) represents the amount of oxygen relative to the amount of organic carbon present in a sample. It is a ratio determined by the formula: OI = (S3/TOC) x 100, where S3 is the amount of carbon dioxide (CO_2) produced during pyrolysis of kerogen (mg CO_2/g rock) and TOC is the total organic carbon, in grams.*

Table 2. *Methane adsorption isotherm for the Gothic shale at 5390.8 feet (1643.1 m), Aneth Unit No. H-117 well. See figure 11 for gas versus pressure plots of methane adsorption data.*

Dry Basis		**TOC = 4.42%**	
Sample Weight = 224.61 g		As-Received Moisture = 1.35%	
Particle Size = < 12 Mesh			
Temperature = 121.0ºF (49.4ºC)			
Methane Adsorption			
Pressure		Gas Content (Dry Basis)	
(psia)	(MPa)	(scf/ton)	(scc/gm)
37	0.26	6.9	0.22
75	0.52	12.1	0.38
124	0.85	17.7	0.55
201	1.39	25.5	0.80
287	1.98	32.8	1.02
376	2.59	40.2	1.25
471	3.25	45.0	1.40
561	3.87	49.0	1.53
662	4.56	51.2	1.60
Langmuir Coefficients		**$V_L = 89.1 * P_L / (P_L + 475.7)$**	
P_L		V_L (Dry Basis)	
(psia)	(MPa)	(scf/ton)	(scc/gm)
475.7	3.28	89.1	2.8

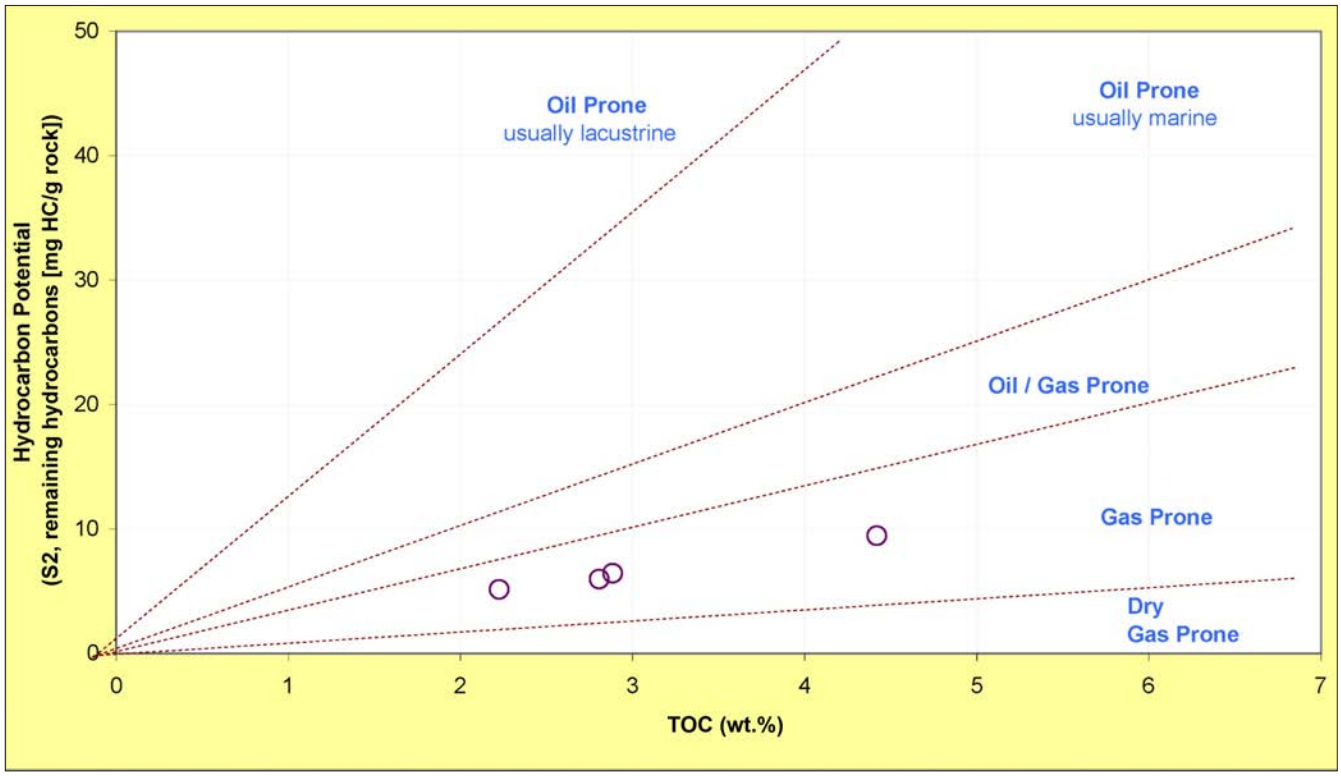

Figure 10. *Kerogen quality determination of the Gothic shale from total organic carbon (TOC) and programmed pyrolysis data. The data indicate the Gothic contains gas-prone kerogen.*

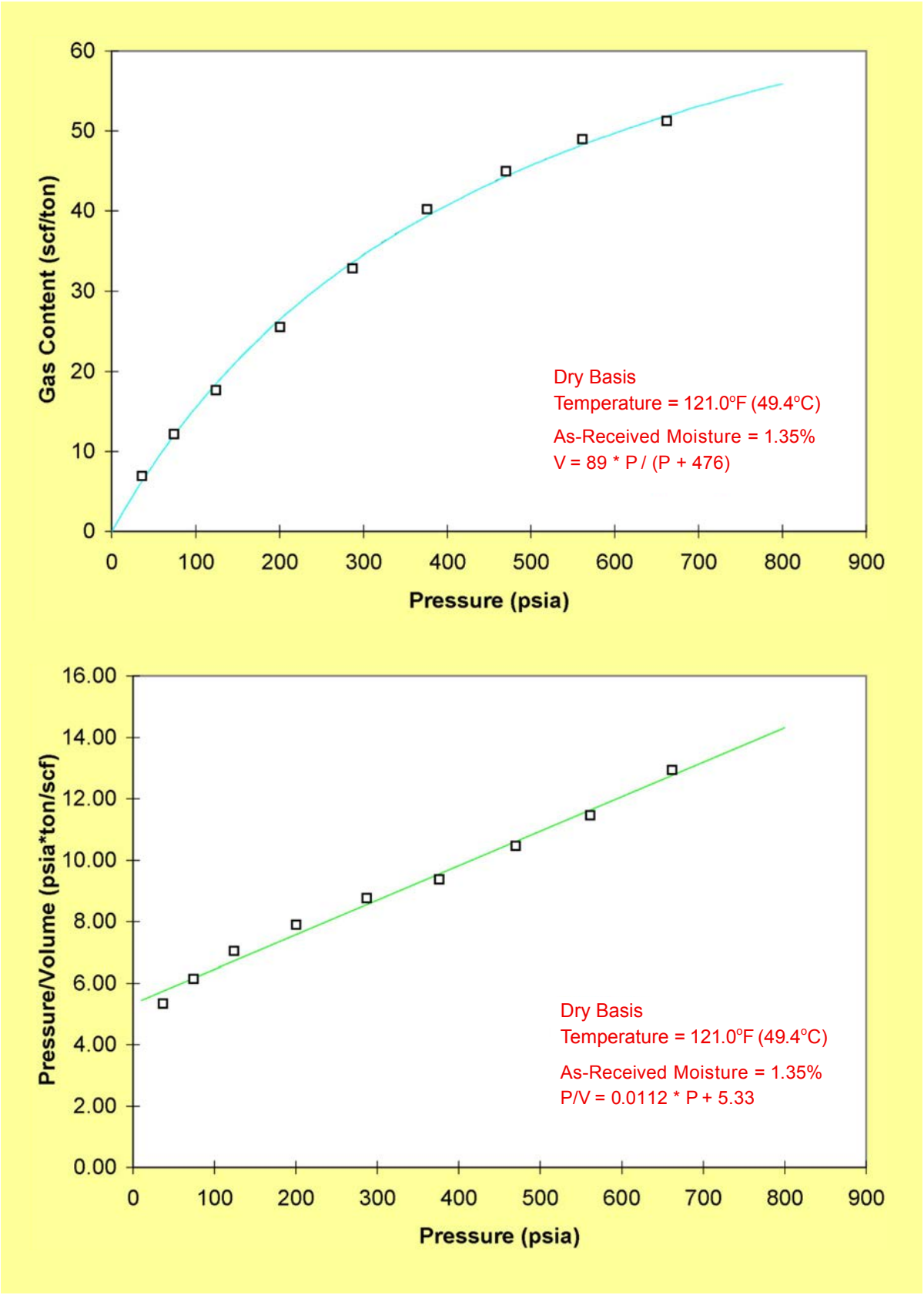

Figure 11. *Methane adsorption for the Gothic shale, sample from 5390.8 feet (1643.1 m), Aneth Unit No. H-117 well.* ***A.*** *Methane adsorption isotherm.* ***B.*** *Adsorption Langmuir plot. Volume (V) = standard cubic feet per ton (scf/ton); pressure (P) = pounds per square inch absolute (psia).*

ranges from 6.9 to 51.2 standard cubic feet per ton (0.22–1.60 scc/gm) at pressures from 37 to 662 psia (0.26–4.56 MPa).

X-ray fluorescence (XRF) and X-ray diffraction (XRD) analyses were also performed on the Gothic core. XRF data for 2-foot (0.6 m) intervals over the length of the core (seven samples) show averages of 41% silicon dioxide, 26% calcium oxide, 10% aluminum oxide, 7% iron oxide, 5% magnesium oxide, 4% potassium oxide, and 3% sulfur trioxide plus various small amounts of trace oxides. Semi-quantitative XRD analysis from five selected intervals was used to define clay composition and clay expandability, and to build log correlations. Certain shale lithofacies can only be verified by XRD analysis. XRD results from bulk and oriented (clay fraction dominant) samples are shown on figure 12. All data are referenced to the magnitude of the quartz peak. Offsets are imposed on the data for the purpose of comparison. The bulk analysis (powder) plot (left) shows the consistency of mineralogical composition over the range of the core. The indistinct illite peak is consistent as are the strong quartz, calcite, and dolomite peaks. The individual sample plots (right),

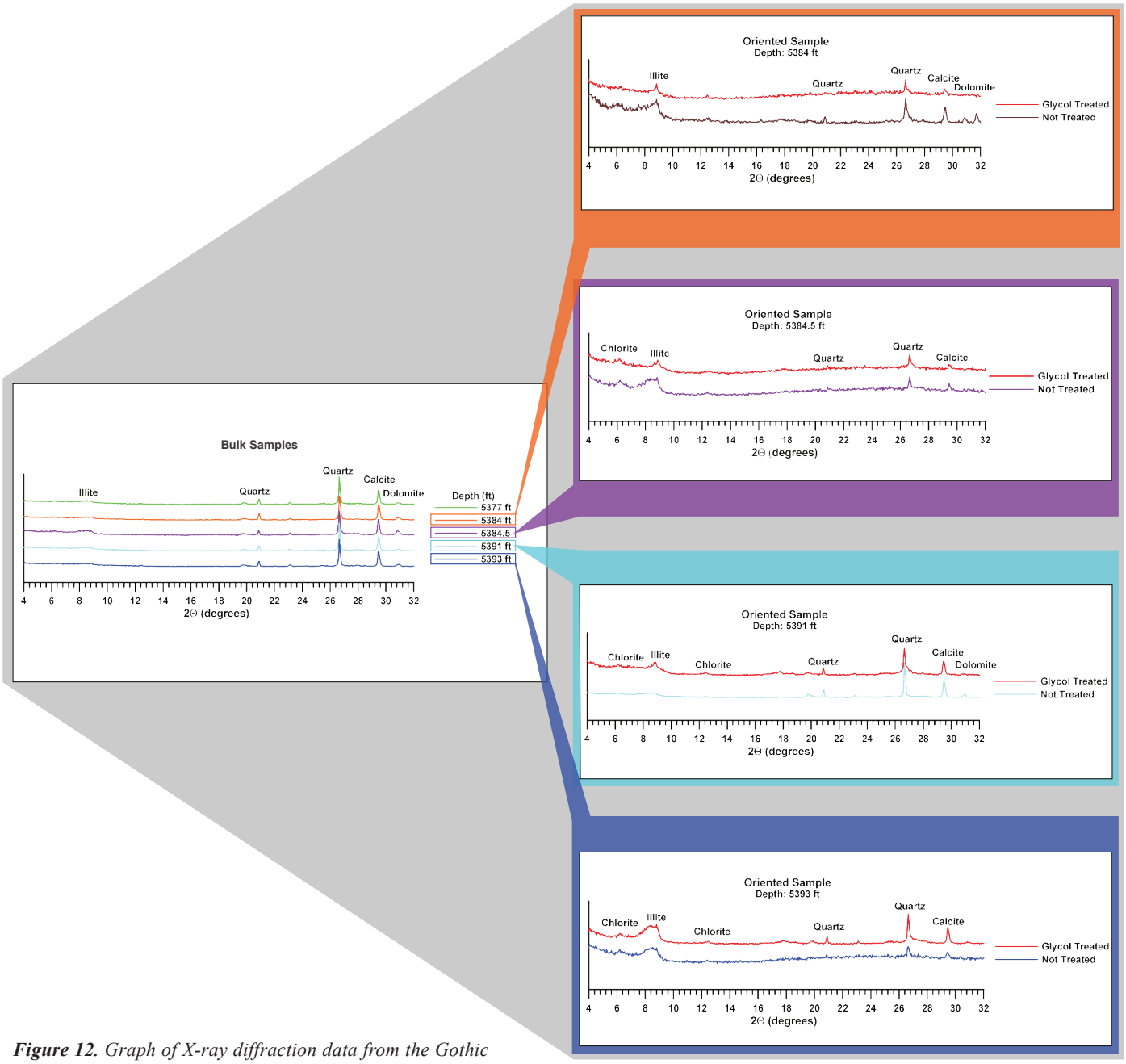

Figure 12. *Graph of X-ray diffraction data from the Gothic shale, Aneth Unit No. H-117 well.*

except for the sample from 5377 feet (1639 m), illustrate the difference between the glycol-treated samples and non-treated samples. Glycol is used only to enhance the peaks of clay minerals, particularly smectites. XRD analysis of the glycol-treated samples in some cases resulted in a definite illite peak whereas in other cases increased the existing illite peak. For example, the non-treated plot for the sample from 5391 feet (1643 m) shows only a slight hint of an illite peak; however, the glycol-treated sample shows a small but distinct illite peak. The other samples show well-defined, non-glycol-treated illite peaks that are enhanced when they were treated with glycol, especially the sample from 5393 feet (1644 m). In all cases the presence of a small percentage (approximately 10%) of illite as well as chlorite and expandable clays (smectites) is inferred.

Petrography

Petrographic analysis of the Gothic shale of the Aneth Unit No. H-117 core reveal four principal lithotypes: (1) argillaceous shale, (2) argillaceous mudstone (mudstone by definition lacks the fine laminations or fissility of shale though having the same texture and composition), (3) silty calcareous-argillaceous mudstone, and (4) phosphatic argillaceous mudstone (Mary Milner, formerly with TerraTek – A Schlumberger Company, written communication, 2009). Although micropores and fractures are present, these lithotypes provide an excellent seal for the hydrocarbons in the Desert Creek reservoir below. Argillaceous shale and mudstone deposited in offshore marine environments are the best seals, whereas the shallow, nearshore silt-rich mudstones tend to be more brittle. The silt-rich mudstones are thin compared to the argillaceous shale and mudstone lithotypes, but because of their brittle nature they have potential for shale-gas and shale-oil production in the region (Chidsey, 2016). Finally, hydrocarbons generated in the Gothic may have charged adjacent, isolated porous dolomite units in the lower Ismay (Bereskin and others, 2010).

Petrographic Methods

Thin-section and scanning electron microscope (SEM) analyses are fundamental to petrological description. Thin-section analyses of Gothic shale samples were used for petrological description of the lithofacies and to establish a baseline correlation of petrophysical properties related to the geologic/petrologic descriptions. They served as a screening tool for important seal-parameter investigations such as diagenetic alteration, cementation, and fracture fills. SEM analysis involves high-magnification imaging of small, representative samples, and is used to identify clay morphology, kerogen location, and pore-throat characterization. Thin-section and SEM analyses show the Gothic shale contains abundant carbonates and clays combined with substantial cementation/compaction creating a high-quality seal.

Two other techniques used are laser scanning confocal microscopy (LSCM) and backscattered electron imaging (BSE). LSCM is a technique for obtaining high-resolution optical images with depth selectivity. The key feature of confocal microscopy is its ability to acquire in-focus images from selected depths, a process known as optical sectioning. Images are acquired point-by-point and reconstructed with a computer, allowing 3-D reconstructions of topologically complex objects. For opaque specimens this is useful for surface profiling (Fredrich, 1999). The BSE is a technique for obtaining high-resolution electron images that show compositional contrast and structural details (De Winter and others, 2009). Backscattered electrons have higher energies than secondaries and are produced when electrons from the primary beam are "bounced" back out of the sample by elastic collisions with atoms. The number of electrons a given material backscatters is proportional to the mean atomic number of the component elements. Materials composed of larger, heavier atoms backscatter more electrons, producing brighter gray tones in the images than less dense materials (differences in average atomic mass of 0.1 amu can be resolved). Backscattered electrons thus produce an image that is related to material composition, providing both spatial and chemical information on mineral and organic matter distribution. Additional details on BSE methods and Gothic shale examples are provided in Heath and others (2011).

Argillaceous Shale

Argillaceous shale in the Gothic shale shows weak laminations defined by micas and compacted cherty microfossils (figure 13A). Shale contains silt-sized calcite particles. The argillaceous shale matrix also supports dispersed, medium silt grains and compacted cherty microfossils. Such forms are characteristic throughout this interval of Gothic shale, and commonly indicate microcrystalline quartz as a matrix cement. Reflected ultraviolet (UV) light display swarms of intercrystalline micropores (figure 13B). SEM images of argillaceous shale display distinct grain orientation (figure 13C). Compacted packets of clays are the main textural feature, separated by planar parting surfaces. The clay-rich matrix hosts numerous micropores; authigenic pyrite is ubiquitous. Shale matrix has wavy parting planes between clay packets (figure 13D). Replaced microfossils are lined with kerogen residue. Matrix clays are likely illite and/or mixed layer illite-smectite. The matrix also shows unaltered and altered carbonaceous material (figure 13D).

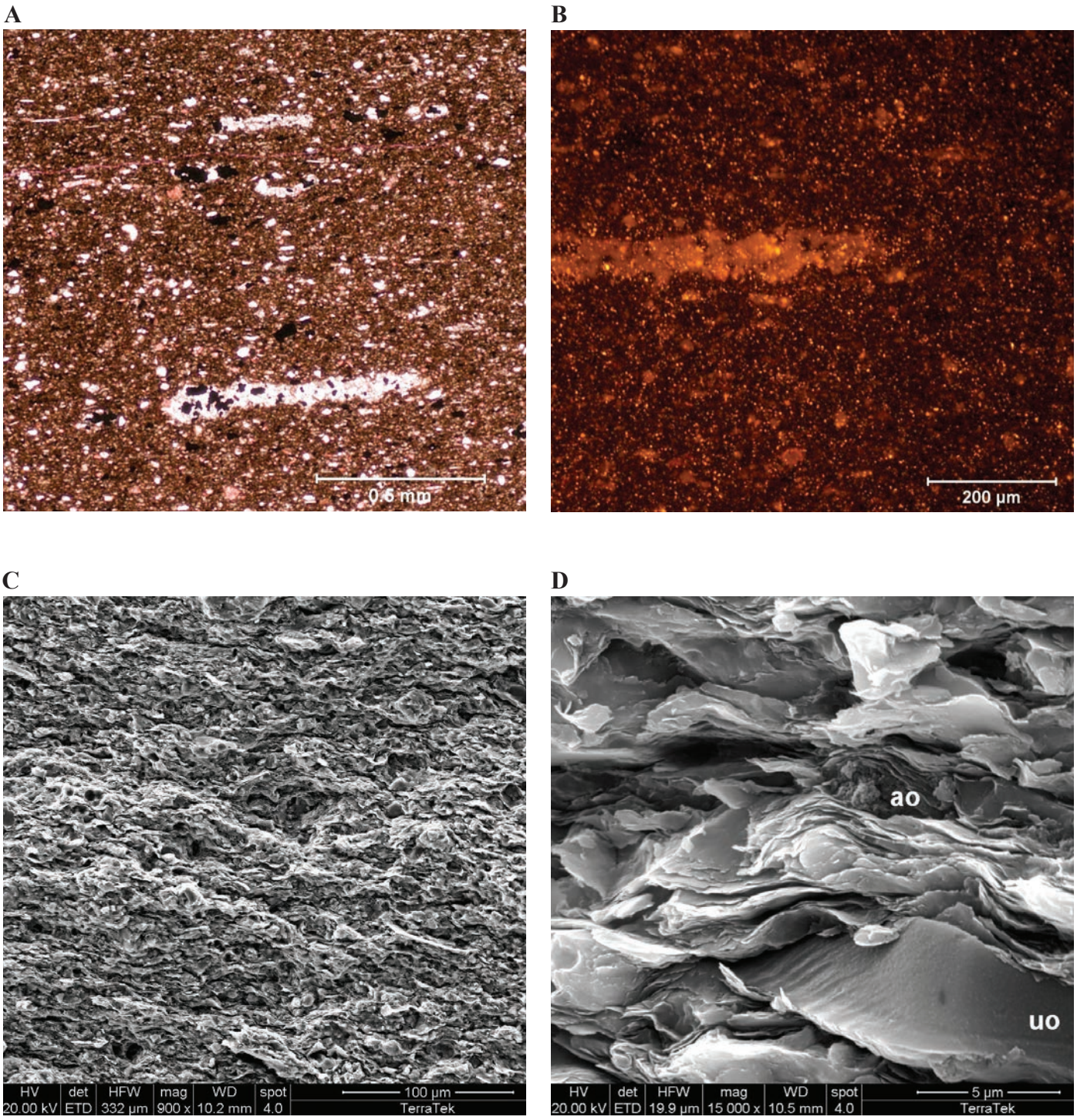

Figure 13. *Argillaceous shale lithotype in the Gothic shale from 5382.8 feet (1640.7 m), Aneth Unit No. H-117 well.* ***A.*** *Photomicrograph of argillaceous shale lithotype showing weak laminations defined by micas and compacted cherty microfossils (white, lower right) (plane light). Pink specks in the matrix are stained, silt-sized calcite particles.* ***B.*** *Reflected UV light with rhodamine filter showing a compacted cherty microfossil (grain at center) in the argillaceous shale matrix and swarms of orange pinpoints that indicate intercrystalline micropores. Brighter fluorescence inside the microfossil is attributed to mineral fluorescence.* ***C.*** *SEM overview of argillaceous shale highlighting distinct grain orientation.* ***D.*** *SEM matrix detail showing unaltered and altered carbonaceous material. The smooth particle at lower right (uo) represents a discrete carbonaceous grain with little alteration. At top center, a particle representing a different class of organics, embedded between clay flakes (ao), displays an unclear, rough texture.*

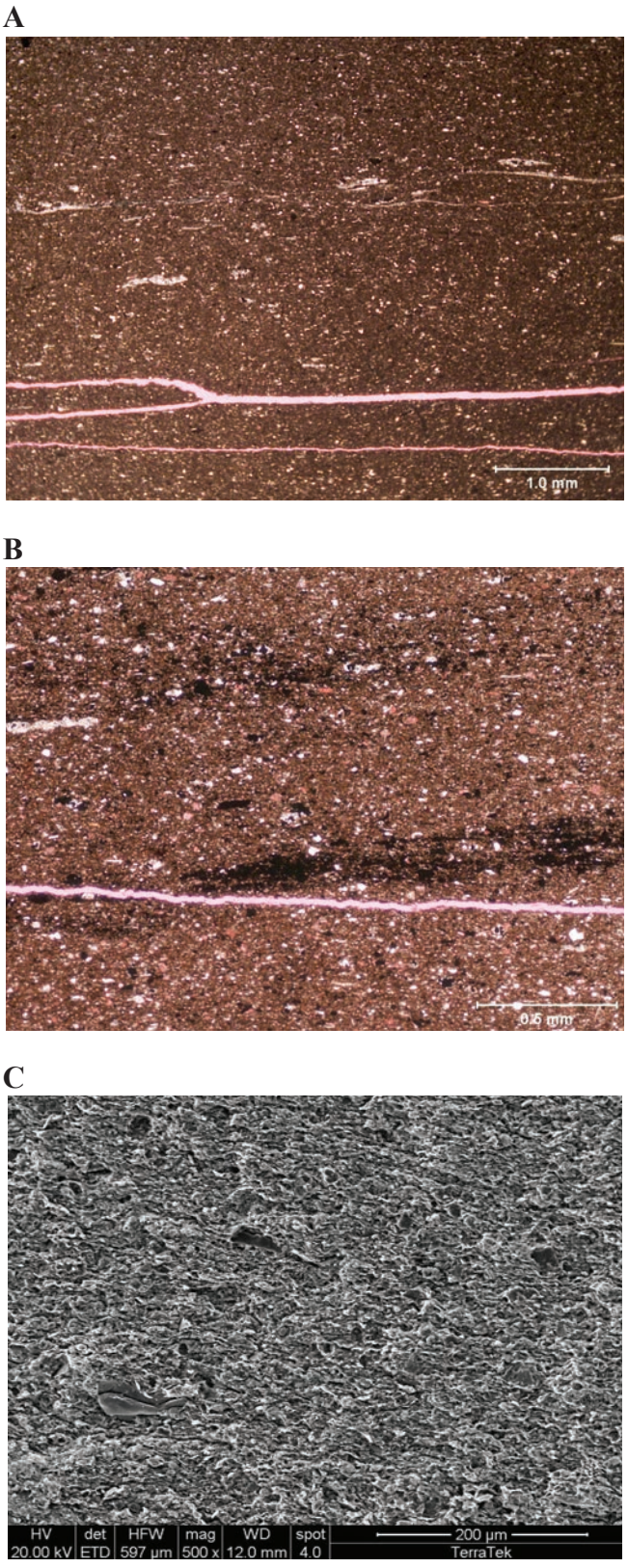

Figure 14. *Argillaceous mudstone lithotype in the Gothic shale from 5379.4 feet (1639.6 m), Aneth Unit No. H-117 well.* ***A.*** *Photomicrograph of argillaceous mudstone shown at low magnification (plane light). The magenta lines at the bottom of the image are induced stress-release fractures.* ***B.*** *Same image as 14A at slightly higher magnification. Black streaks are pyrite concentrated parallel to bedding.* ***C.*** *SEM overview of texture in uniform, non-laminated argillaceous mudstone.*

Argillaceous Mudstone

Argillaceous mudstone lithotypes in Gothic shale show a clay matrix supporting a few elongate chert stringers (figure 14A). These likely represent microfossils, scattered pyrite, and silt, as well as silt-sized calcite crystals. Pyrite is concentrated parallel to bedding (figure 14B). The SEM overview of this texture shows uniform, non-laminated argillaceous shale (figure 14C). A few siliceous and calcareous fragments float in a matrix of crenulated clays. LSCM images of a surface perpendicular to bedding in argillaceous mudstone show topography in corresponding oblique and map views on figure 15. The map view shows green, yellow-orange, and red fluorescing material at different magnifications. Red material is typically spherical and probably co-located with pyrite framboids. Green fluorescing material is the most abundant organic material, reflective of a primary depositional process that distributed the organic material. BSE images of argillaceous mudstone show the presence and distribution of pyrite, dolomite, calcite, smectite, illite, chlorite, and plagioclase (figure 16).

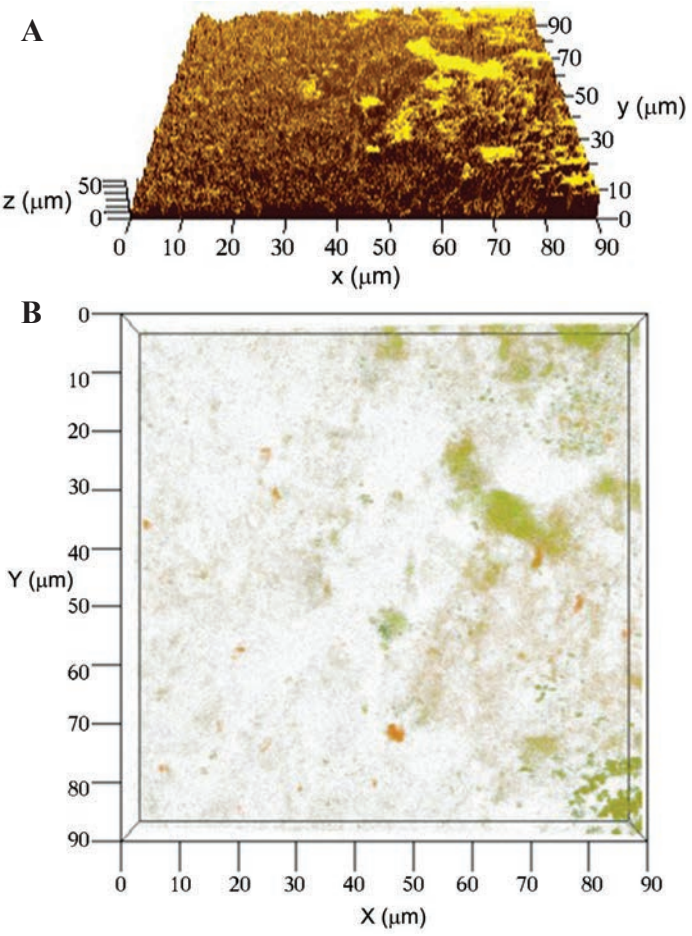

Figure 15. *Medium magnification of corresponding LSCM images of a surface broken perpendicular to bedding in the Gothic shale from 5380.0 feet (1638.8 m), Aneth Unit No. H-117 well.* ***A.*** *Image showing topography in an oblique view.* ***B.*** *A relatively high-resolution image of green, yellow-orange, and red fluorescing material.*

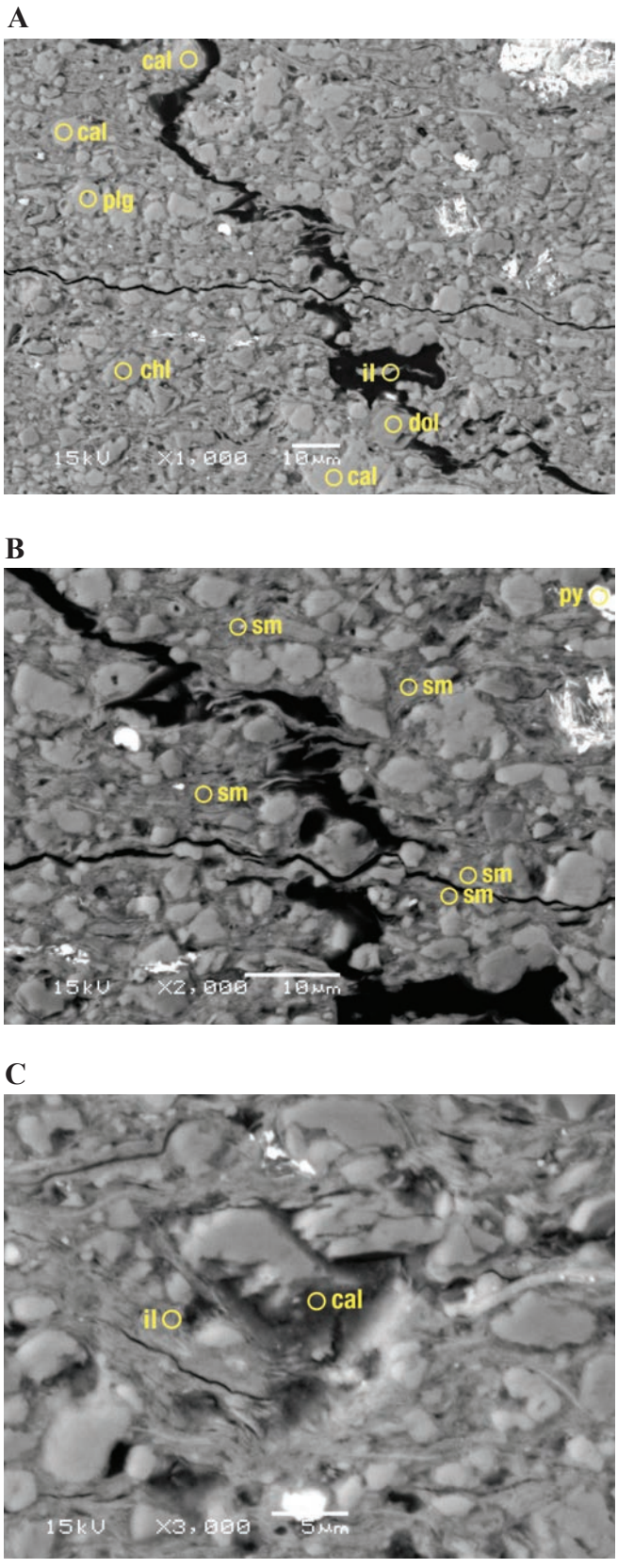

Figure 16. *Backscattered electron images of the Gothic shale from 5387.1 feet (1642.0 m), Aneth Unit No. H-117 well, from low* ***(A)*** *to medium* ***(B)****, to high magnification* ***(C)****, showing various mineral constituents (cal = calcite, dol = dolomite, plg = plagioclase, il = illite, chl = chlorite, sm = smectite, py = pyrite).*

Silty Calcareous-Argillaceous Mudstone

Silty calcareous-argillaceous mudstone consists of finely disseminated carbonaceous material and abundant silt grains (figure 17A). The dominant textural components in the matrix are quartz silt, silt-sized calcite, mica flakes, and authigenic pyrite, which "float" in a predominantly clay matrix (figure 17B). SEM images of calcareous-argillaceous mudstone confirm the presence of many calcite particles and quartz silt grains. Cement-coated clay flakes preserve the microporous structure (figure 17C). Elongate pores are parallel to parting planes. The micropore network consists of pores having sizes from 2 to 10 microns, which are flattened in shape. Carbonaceous material is often preserved and commonly associated with pyrite (figure 17D). Intercrystalline porosity developed through alteration of organics.

Phosphatic Argillaceous Mudstone

Phosphatic argillaceous mudstone is a typical component of the Gothic shale. Flattened, amalgamated phosphate pellets are common (figure 18A). Phosphatic argillaceous mudstone also includes compacted chert, siliceous fossils, detrital micas, and flattened pellets in a mixed siliceous/argillaceous matrix with a siliceous cement component (figures 18B). Significant and abundant micropores may also be present within this matrix. Micropores appear under UV light (figure 18B). SEM images of phosphatic, argillaceous mudstone show the clay packets that make up the matrix are separated along parting surfaces, contributing to a fissile texture (figure 18C). Flattened phosphatic/organic pods have granular internal textures along horizontal parting planes (figure 18D). BSE images of phosphatic argillaceous mudstone show pyrite, dolomite, calcite, quartz, smectite, and illite/smectite (figure 19).

Analysis of Natural Fractures

Fractures that could connect Desert Creek reservoir rock through the Gothic shale are a potential concern for hydrocarbon and CO_2 leakage. Fracture analysis includes the evaluation of natural and induced fracture systems, fracture orientation (vertical, inclined, or horizontal), and mineral composition of fracture fill. Typical tabulated data from the fracture analysis include general fracture type, fracture dip orientation, type of mineral fill, type of oil stain, apparent fracture dip, fracture porosity, fracture spacing, and fracture intensity. Fractures present in the Gothic will be an important factor in CO_2 containment. Natural fractures in the Aneth Unit No. H-117 core include three individual inclined shear fractures or fracture zones and one horizontal shear fracture. Fractures are slickensided and partially mineralized.

Flat, horizontal disc fractures were observed in the Gothic shale. These fractures are induced during the drilling process and exhibit a radial plume pattern indicating there is likely not a large differential stress. Disc fractures that have plumes with

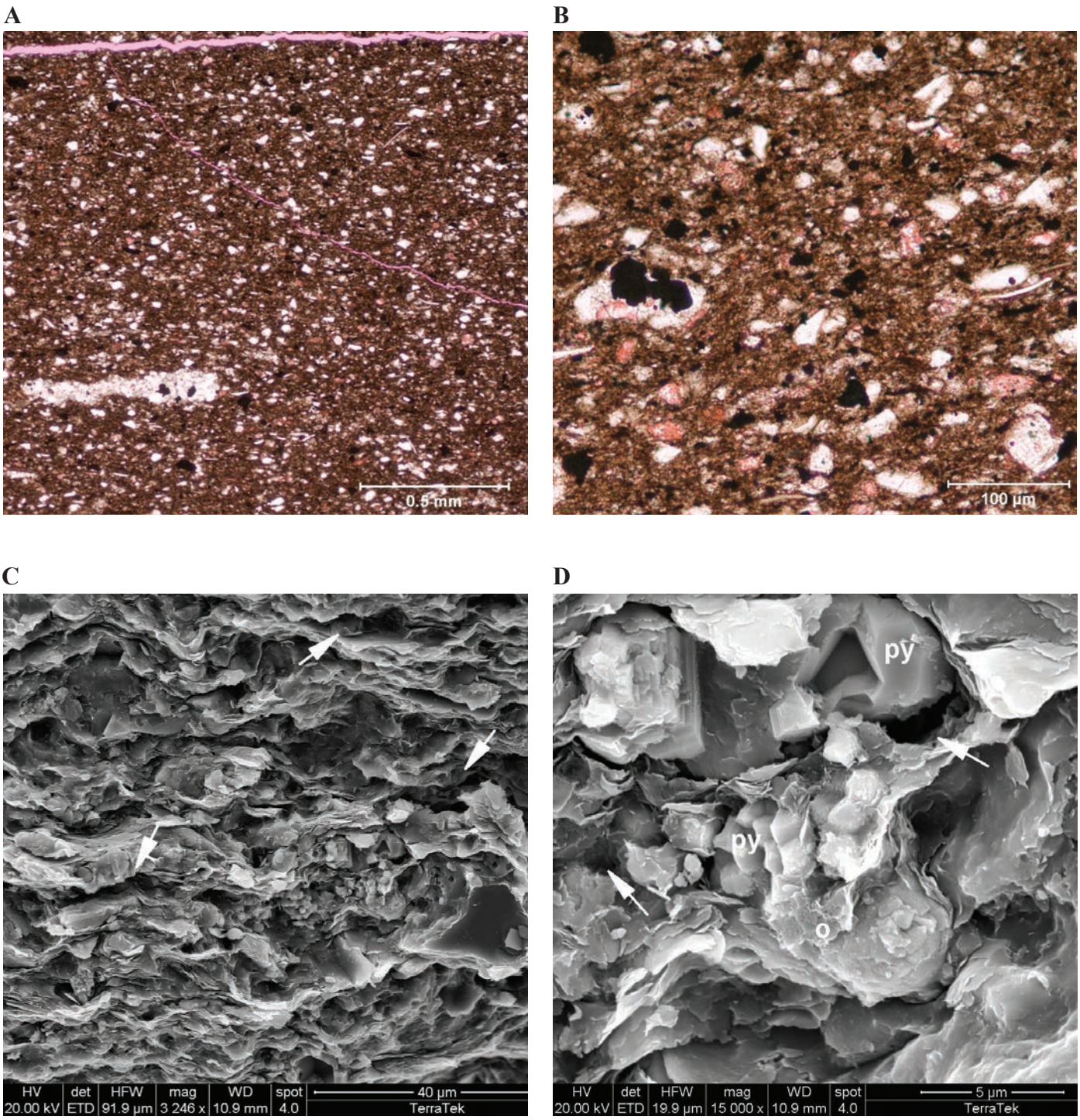

Figure 17. *Silty calcareous-argillaceous mudstone lithotype in the Gothic shale from 5386.9 feet (1641.9 m), Aneth Unit No. H-117 well.* ***A.*** *Photomicrograph of silty calcareous-argillaceous mudstone with induced fracture at the top of the image (magenta) (plane light). Finely disseminated carbonaceous material is visible in the matrix, as are abundant silt grains, calcite crystals (pink), and pyrite. Note cherty microfossil at bottom of image.* ***B.*** *Photomicrograph showing matrix detail highlighting dominant textural components (plane light). Quartz silt, silt-sized calcite (red), mica flakes, and authigenic pyrite float in a predominantly clay matrix.* ***C.*** *This medium magnification SEM view of the matrix shows elongate pores parallel to parting planes (arrows). The micropore network is also visible, consisting of voids with sizes from 2 to 10 microns, and flattened in shape.* ***D.*** *Image illustrates a common association of pyrite with carbonaceous material. The perforated flakes of organics (o) surround pyrite crystals (py). Intercrystalline porosity (arrows) is believed to have developed through alteration of organics.*

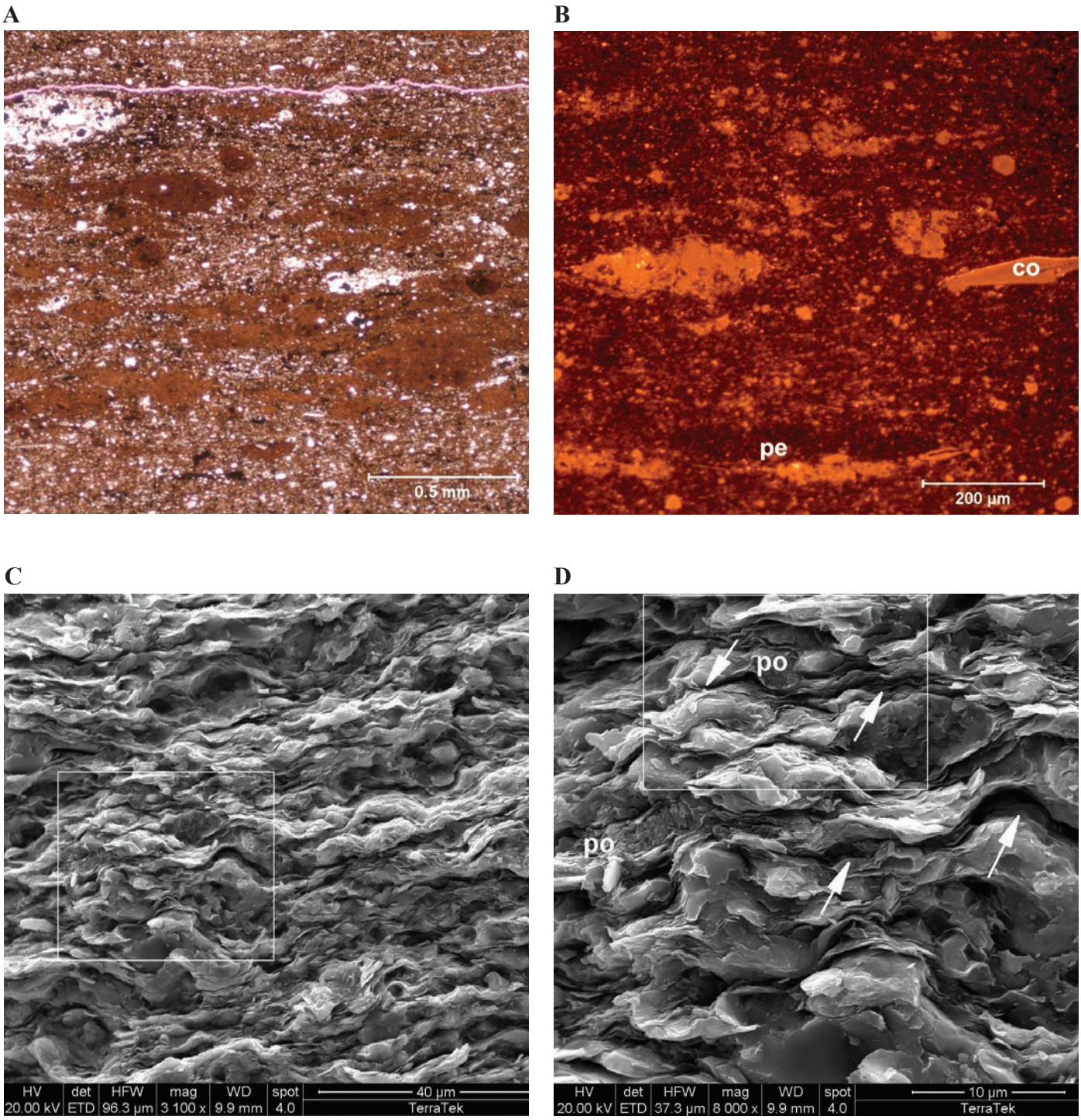

Figure 18. *Phosphatic argillaceous mudstone lithotype in the Gothic shale from 5390.8 feet (1643.1 m), Aneth Unit No. H-117 well.* ***A.*** *Photomicrograph (plane light) of overview showing flattened, amalgamated pellets (lighter brown), which SEM show to be phosphatic. The matrix overview highlights compacted siliceous forms (white) composed of chert, and flattened pellets in a mixed siliceous/argillaceous matrix. The lighter brown matrix color and abundance of siliceous fossils, as well as phosphatic pellets suggest a siliceous matrix cement component.* ***B.*** *Closer view showing microfossils, micas, a pellet (pe) and a conodont (co) supported by argillaceous matrix under reflected UV light. Note the matrix micropores appearing as bright orange dots. Dull orange is mineral fluorescence. (Reflected UV light with zcrhodamine filter).* ***C.*** *Medium magnification SEM view of phosphatic, argillaceous mudstone. Clay packets that make up the matrix are separated along parting surfaces, contributing to a fissile texture. The sample splits easily along closely spaced (<1 mm), brittle, wavy partings. The boxed area is enlarged in the image 18D.* ***D.*** *SEM detail of part of the image 18C highlighting two flattened phosphatic/organic pods (po) with granular internal texture arranged along horizontal parting planes (arrows).*

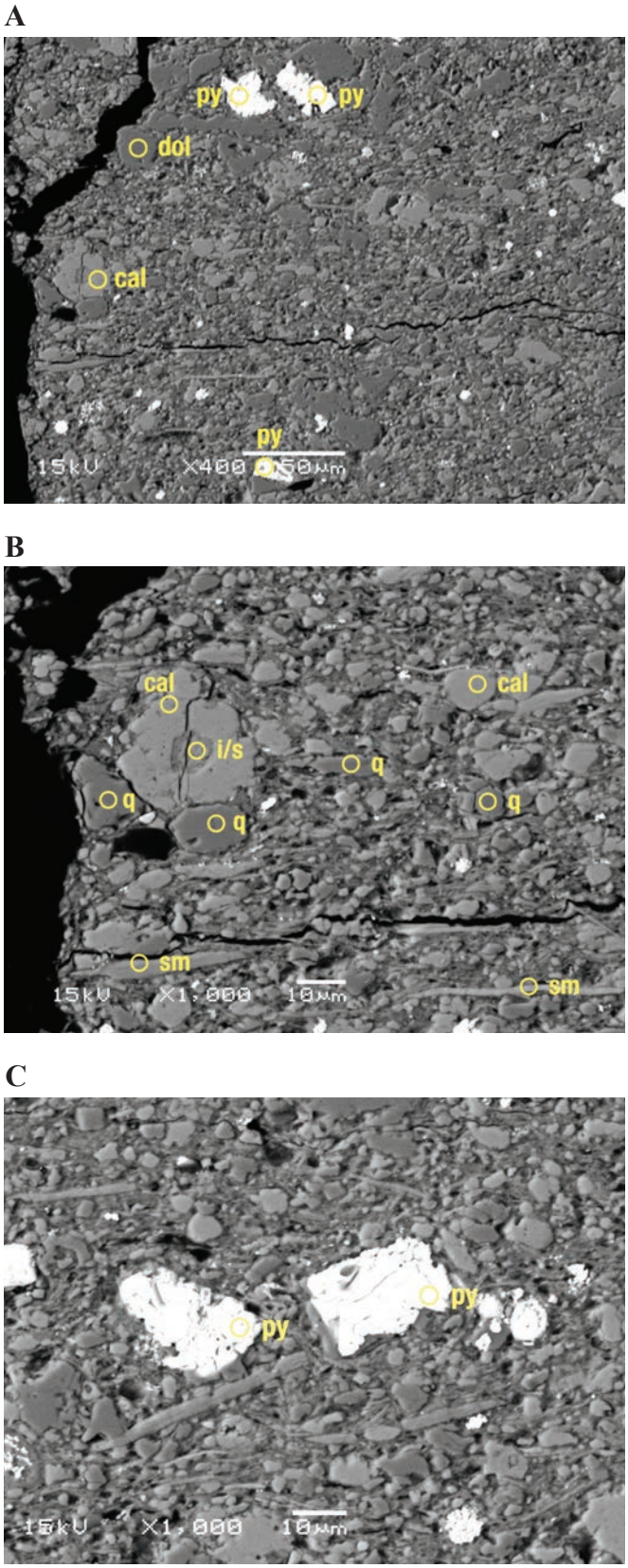

Figure 19. *Backscattered electron images of the Gothic shale from 5392.4 feet (1643.6 m), Aneth Unit No. H-117 well, from low* ***(A)*** *to medium* ***(B)****, to high magnification* ***(C)****, showing various mineral constituents (cal = calcite, dol = dolomite, q = quartz, i/s = illite/smetite, sm = smectite, py = pyrite).*

significant directionality are indicative of high differential stresses; this was not observed in these cores. The plumes on the disc fractures do not seem to be exceptionally asymmetric, sometimes without orientation and without a strongly defined axis of propagation. These characteristics usually suggest that the present-day horizontal stress anisotropy is not strong, and therefore, hydraulic fractures in the formation could be diverted by larger fracture systems and structural heterogeneities. A limited number of inclined disc fractures suggest that the stress axes are not aligned with present-day gravity; however, we infer that these are likely caused by the influence of local bedding deformation rather than stress realignment.

Inclined shear fracture zones (figure 20), possible permeability pathways, are undulous and contain multiple fracture surfaces; overall dip ranges from 30° to 44°. Slickenlines rake obliquely across the dip of the shear planes, and are probably parallel on successive planes. They suggest significant horizontal tectonic compression at some point during the geologic history of the strata. These sub-horizontal shear planes were observed in both the Gothic shale and upper Desert Creek zone. The inference is that this may be a zone of incipient or limited displacement.

Thin sections and LSCM images reveal both extension and shear fractures (figure 21). Dilational jogs and crack-seal textures are visible in the images. Maximum principal compressive stress is vertical and the sense of shear is dextral.

Fluorescent organics are co-located with mineralization in fractures. Microprobe analysis indicates that carbonates and sulfates dominate fracture mineralization (see BSE images on figure 21). Fracture mineralization contains microporosity and does not show strong crystal orientation. Vertical fractures are extensional. Cross-cutting relationships between vertical and subhorizontal shear fractures could not be discerned; perhaps the mineralization occurred synchronously in the two types of fractures.

This evaluation shows that organic material is co-located with fracture mineralization, as well as in the argillaceous mudstone (figure 15), in the Gothic shale. Organics and carbonate might be affected geochemically by CO_2-rich fluids. Within the matrix, micropores, and fractures, CO_2 generated from within the Gothic or as part of the CO_2-rich fluid phase migrating from the Desert Creek reservoir may cause (1) organics to become mobilized on a microscale/molecular scale, (2) carbonates to dissolve, (3) creation of new fractures, or (4) the precipitation of the carbon-bearing mineral dawsonite ($NaAlCO_3(OH)_2$). These processes would be dependent on the temperature, pressure, and other conditions within the Gothic and Desert Creek.

Induced dehydration features/fractures are not present in the Aneth Unit No. H-117 core. However, if they are present elsewhere in the Gothic shale the potential exists for creation of

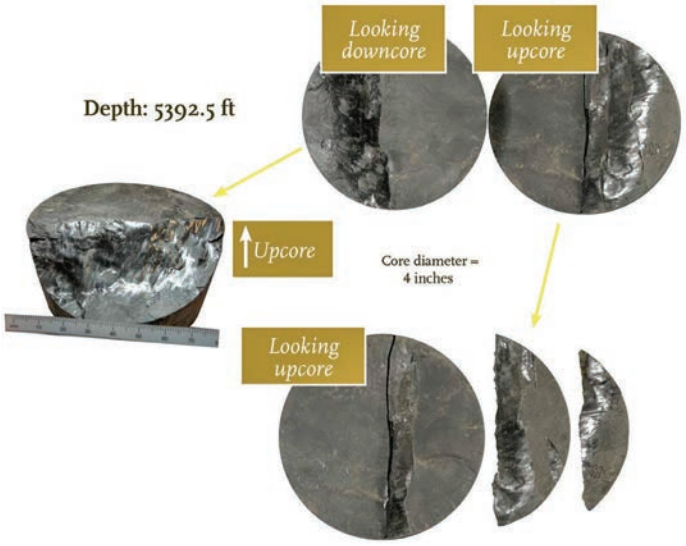

Figure 20. *Inclined shear fracturing (various views) with slickensides in the Gothic shale core, 5392.5 feet (1643.6 m), Aneth Unit No. H-117 well (shown in the detailed images, on figure 21, generated from an assortment of microscopic techniques).*

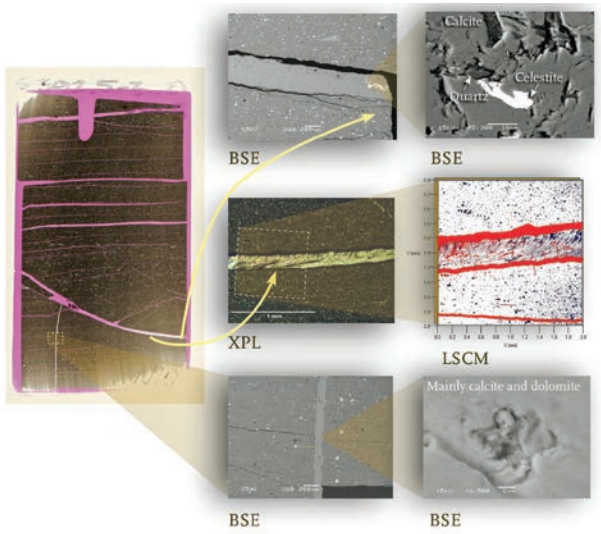

Figure 21. *Inclined shear fracture zone from 5392.30 to 5392.50 feet (1643.57–1643.63 m) (core shown on figure 20) displayed on various backscattered electron (BSE), crossed-polars thin section photomicrograph (XPL), and laser scanning confocal microscopy (LSCM) images at different magnifications derived from the thin section shown on the left.*

fracture zones if separate or dissolved phase CO_2 can affect surface forces of the clay particles and their expanded versus collapsed texture (Andreani and others, 2008). No fractures connecting the Desert Creek reservoir from which CO_2-rich fluids could migrate into the Gothic shale were observed in the Aneth Unit cores.

Petrophysical Properties

Shales are heterogeneous and strongly anisotropic. Sampling along the entire Gothic core interval was of fundamental importance for analysis of any future hydraulic fracturing (that could be required for later CO_2 storage) containment from the Desert Creek zone below.

Basic Reservoir Parameters

Petrophysical measurements were conducted to determine the density, porosity, permeability, saturations (gas, oil, and water), and bound water of the Gothic shale (table 3) (Chidsey, 2016). These measurements are fundamental for seal capacity, as well as gas-in-place and gas productivity evaluations for potential gas shale reservoirs. The tests characterize the gas-filled and the effective porosities, the fluid saturations including mobile hydrocarbons (such as condensates), and the "as received" matrix permeability to gas. Pressure decay permeability measures to 10 nanodarcy accuracy under reservoir net confining stress conditions and permits effective permeability to be measured at residual fluid pressure without moving fluid in the pore system.

Porosity ranges from 2.7% to 3.4% and pressure-decay permeability is no greater than 0.000146 mD. These and other basic matrix petrophysical parameters indicate the Gothic shale is a highly effective reservoir seal.

Mercury Injection Capillary Pressure and Pore Aperture Distributions

The seal capacity of the Gothic shale—the CO_2 column heights retained by capillary pressure—was quantified by mercury injection capillary pressure measurements to understand and predict variations in seal capacity. Capillary pres-

Table 3. *Summary of petrophysical measurements from the Gothic shale, Aneth Unit No. H-117 well.*

Depth (ft)	As Received Bulk Density (g/cm^3)	As Received Grain Density (g/cm^3)	Dry Grain Density (g/cm^3)	Porosity (% of Bulk Volume)	Water Saturation (% of Pore Volume)	Gas Saturation (% of Pore Volume)	Mobile Oil Saturation (% of Pore Volume)	Gas Filled Porosity (% of Bulk Volume)	Bound Hydrocarbon Saturation (% of Bulk Volume)	Bound Clay Water (% of Bulk Volume)	Pressure-Decay Permeability (mD)
5379.40	2.570	2.623	2.648	3.35	19.55	60.61	19.84	2.03	1.14	6.56	0.000146
5382.80	2.561	2.597	2.621	2.72	24.73	50.88	24.39	1.38	1.33	7.01	0.000133
5386.90	2.572	2.615	2.649	3.51	30.07	47.71	22.22	1.67	0.90	7.42	0.000138
5390.80	2.522	2.573	2.614	4.30	36.18	46.05	17.77	1.98	1.47	7.46	0.000141

sure data applications used in our study included (1) determination of pore throat size distribution, and (2) cap rock–seal capacity analysis to predict the height of CO_2 and hydrocarbon columns that can be retained by the seal.

The Gothic shale has very high seal capacity based on mercury injection capillary pressure and pore aperture distributions analysis (figure 22A and 22B). These data show that clay content and high carbonate cementation and/or compaction lead to small pore throat diameters. The Gothic shale should support very large CO_2 or hydrocarbon columns (1500 to 2600 feet [500–860 m]). The sample (the outlier) with the highest seal capacity was from the depth of 5378 feet (1639 m). Heath and others (2011) provide mercury intrusion porosity saturation curves and cumulative and incremental volumetric pore-density distribution curves for the Gothic (and other seals). Compared to other seals in their study, the Gothic shale curves have the highest pressure values for corresponding mercury saturations and the highest breakthrough pressure.

Heath and others (2011) also summarized the frequencies of Gothic pore throat areas and equivalent circular radii from the connected pore networks, pore body volumes, and ratios of pore throat to pore body equivalent circular radii. Peak frequencies occur for the smallest values for pore throat area, radii, and pore body volume, indicating that most of the connections in the pore networks are controlled by the smallest pore throats (Heath and others, 2011).

Geomechanics

Rock mechanic tests were performed to assess the variability of elastic properties and in situ stresses. Shales, in particular, are strongly heterogeneous and anisotropic, and thus their elastic properties are different in the vertical and horizontal directions. This contrast in elastic properties is not directly measured by geophysical well logs, but can have a dominant impact on predictions of in situ stress. Therefore, the evaluation of anisotropic material properties and the in situ stress throughout the core (for example, in situ stress variations with respect to reservoir units and seals) is of fundamental importance. In situ stress analysis of the Gothic shale was conducted to obtain a reasonable profile of the in situ stress tensor (magnitude and orientation). In situ stress analysis and mechanical property measurements provide fundamental data for evaluation of fracture containment when the Desert Creek reservoir below is hydraulically fractured for CO_2 storage. Multistress anisotropy measurements are summarized in table 4 (Chidsey, 2016).

Young's Modulus and Poisson's Ratio

Young's modulus is a measure of the stiffness of an isotropic elastic material. It is defined as the ratio of the uniaxial stress over the uniaxial strain in the range of stress in which Hooke's Law holds. Young's modulus is the ratio of stress, which has units of pressure, to strain, which is dimensionless; therefore, Young's modulus itself has units of pressure. Figure 23 displays vertical dynamic Young's modulus as a function of vertical static Young's modulus (A) and horizontal dynamic Young's modulus as a function of horizontal static Young's modulus (B).

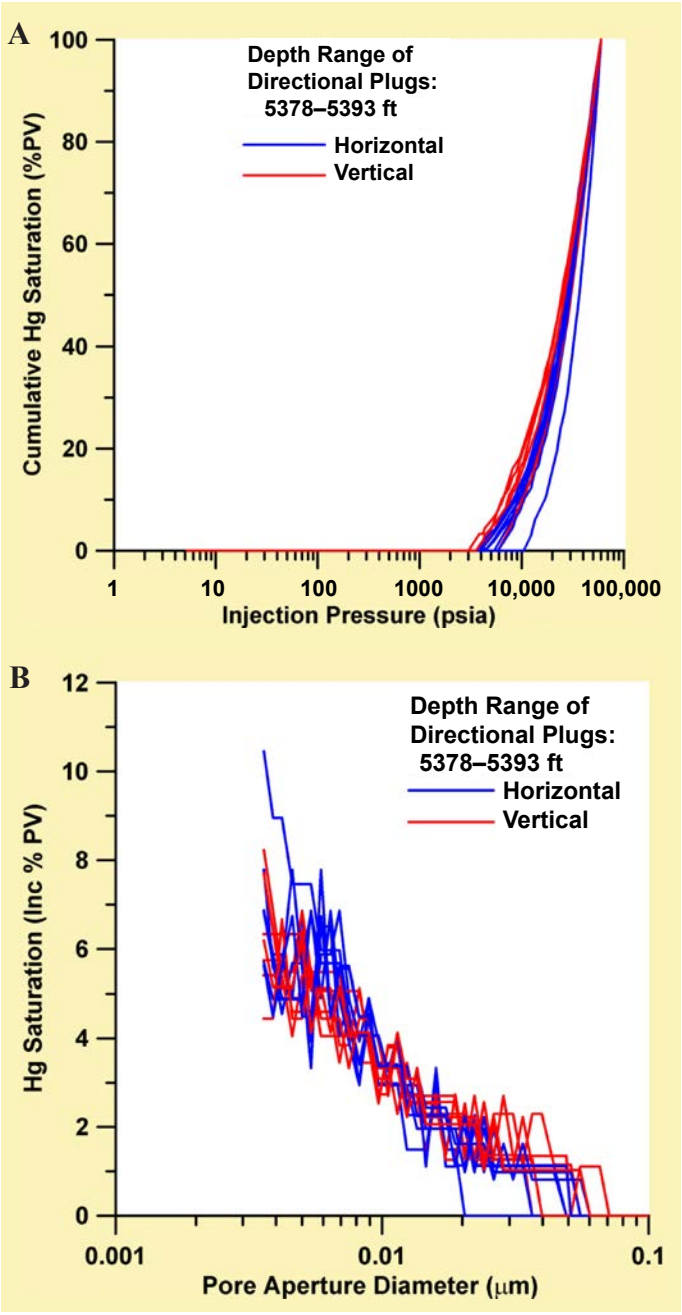

Figure 22. *Mercury injection capillary pressure and pore aperture distributions.* ***A.*** *Cumulative mercury saturation versus injection pressure.* ***B.*** *Mercury saturation versus pore-aperture diameter. All test data and graphs are available from the Utah Geological Survey project files.*

Poisson's ratio compares the contraction or transverse strain (normal to the applied load) to the extension of axial strain (in the direction of the applied load). Figure 24 displays vertical dynamic Poisson's ratio as a function of vertical static Poisson's ratio (A) and horizontal dynamic Poisson's ratio as a function of horizontal static Poisson's ratio (B).

Table 4. *Summary of multistress anisotropy measurements from the Gothic shale, Aneth Unit No. H-117 well.*

Depth (ft)	Orientation	AR Bulk Density (g/cm^3)	Effective Mean Stress (psi)	Young's Modulus – Transverse (psi)	Young's Modulus – Axial (psi)	Poisson's Ratio – Transverse	Poisson's Ratio – Axial	Shear Modulus – Transverse (psi)
5381.20	V	2.568	1994	2.897E+06	5.680E+06	0.186	0.274	1.156E+06
5381.20	45	2.569	1994	2.926E+06	5.648E+06	0.167	0.268	1.164E+06
5381.15	H	2.574	1994	2.913E+06	5.849E+06	0.161	0.273	1.126E+06
5398.80	V	2.283	1994	3.516E+06	3.601E+06	0.191	0.191	1.503E+06
5399.00	45	2.316	1994	3.466E+06	3.638E+06	0.179	0.181	1.458E+06
5398.75	H	2.258	2004	3.597E+06	3.475E+06	0.148	0.150	1.470E+06

Note: transverse – perpendicular to bedding plane, axial – parallel to bedding plane

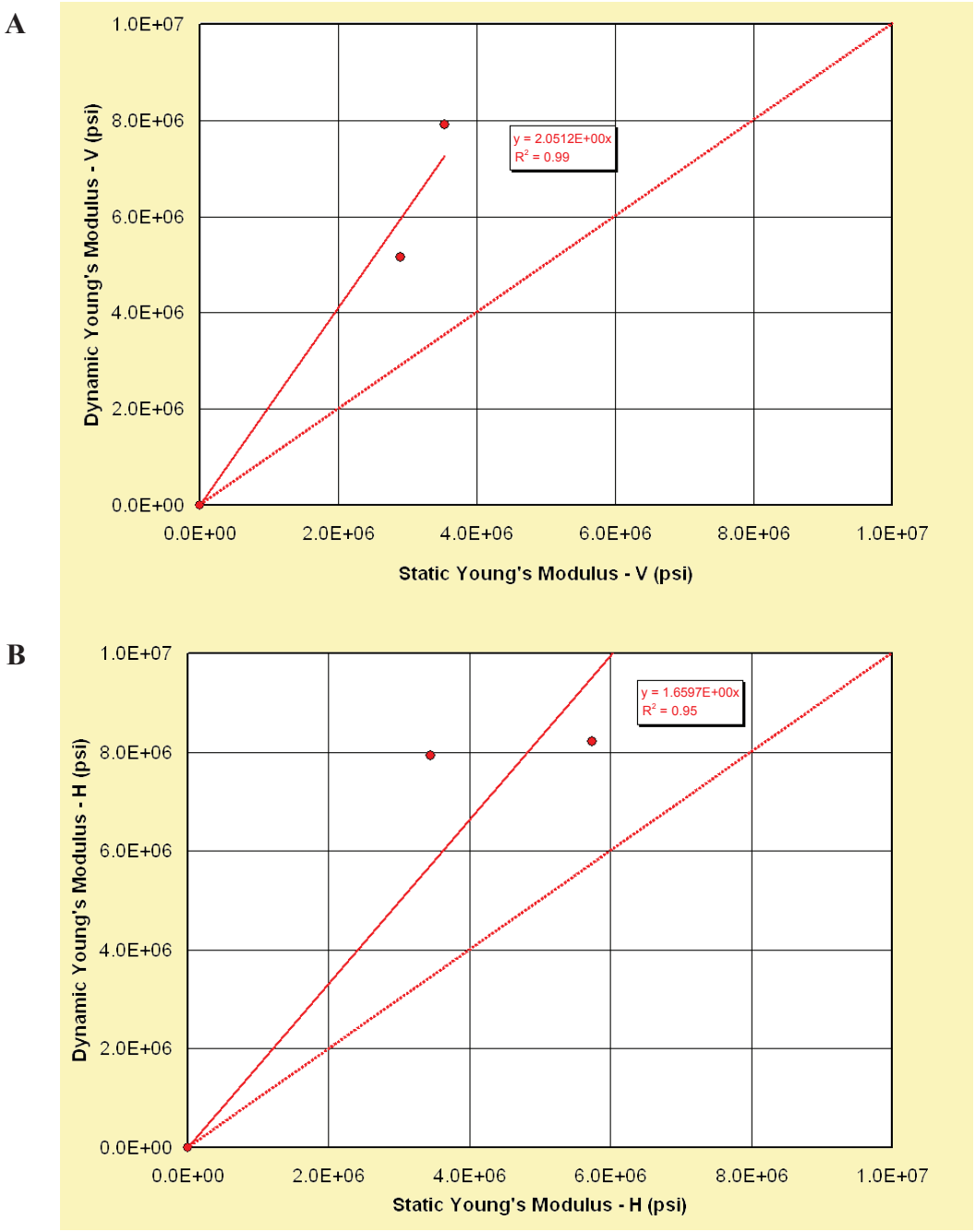

Figure 23. *Young's modulus plots; depth 5381.18 to 5398.85 feet (1643.23–1645.57 m), Aneth Unit No. H-117 well.* ***A.*** *Vertical dynamic Young's modulus as a function of vertical static Young's modulus.* ***B.*** *Horizontal dynamic Young's modulus as a function of horizontal static Young's modulus.*

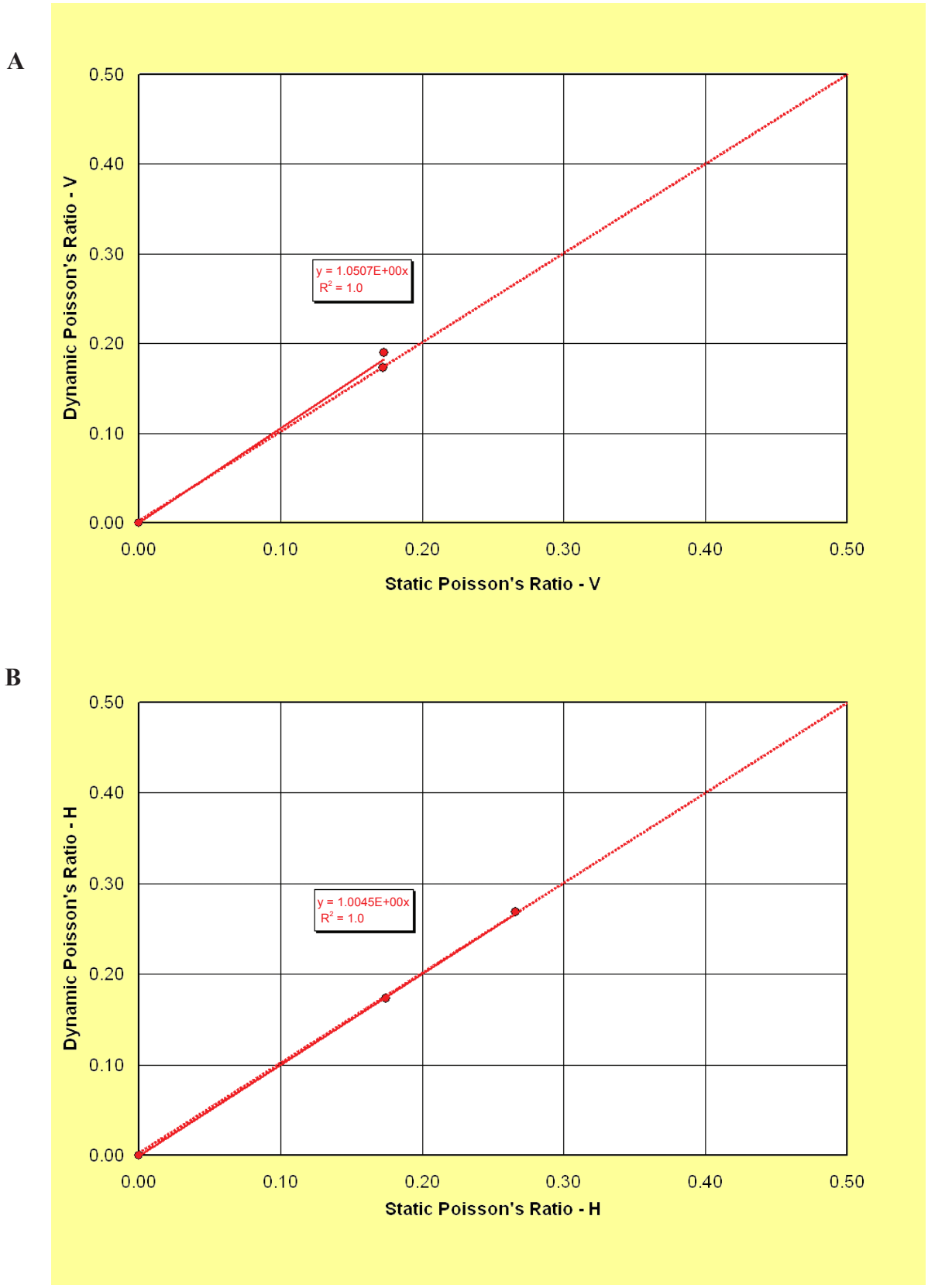

Figure 24. *Poisson's ratio plots; depth 5381.18 to 5398.85 feet (1643.23–1645.57 m), Aneth Unit No. H-117 well.* ***A.*** *Vertical dynamic Poisson's ratio as a function of vertical static Poisson's ratio.* ***B.*** *Horizontal dynamic Poisson's ratio as a function of horizontal static Poisson's ratio.*

These graphs and analysis from Young's modulus and Poisson's ratio suggest that the Gothic shale in the Aneth Unit is not brittle. Therefore, the Gothic is less likely to respond to hydraulic fracturing of the underlying Desert Creek zone.

Compressional Testing

Figure 25A is a plot of axial stress difference versus radial and axial strains, measured during unconfined compression testing. The plot shows the evolution of rock deformation (that is, axial and radial strains) and failure (that is, yield stress, peak stress, and residual strength, when available) during unconfined compression loading. Figure 25B is a plot of axial stress difference versus volumetric strain, measured during unconfined compression testing. The plot shows the evolution of the rock deformation (dilation versus compaction) and the yield stress during unconfined compression loading. Axial stress difference versus axial strain, measured during unconfined compression testing, is displayed on figure 25C. The plot shows the evolution of the axial modulus (Young's modulus) during unconfined compression loading. The averaged radial strain versus axial strain, measured during unconfined compression testing, is shown on figure 25D. The plot shows the evolution of the transverse modulus (Poisson's ratio) during unconfined compression loading.

High-resolution, continuous strength profiling provides a continuous unconfined compressive strength (UCS) measurement along the length of the Aneth Unit No. H-117 core to determine the rock heterogeneity, assess fracture density (if fractures were present), and provide quantitative data to locate zones of potential weakness in the Gothic shale. A continuous strength profile was conducted on the Gothic using the TerraTek TSI™ scratch test system. The system consists of a moving cart with a sample holder and a loading fixture capable of "scratching" the rock sample and measuring the horizontal force (in the cutting direction) and the vertical force (normal to the cutting surface) under conditions of constant depth of cut (0.5 mm) and constant cut velocity (5 mm/second). The UCS profiles along the core show a relatively uniform homogenous Gothic shale package ~20,000 psi (137,900 kPa) (figure 26). A few fractures, likely induced, show up as distinct shifts on the profiles. Compressional testing suggests the potential for some degree of hydraulic fracture containment. The relatively high UCS indicates that throughout the geologic past the Gothic has been able to withstand "high loads" without sustaining significant natural fractures. Thus, the Gothic would likely also withstand the impact of hydraulic fracturing should it be conducted in the Desert Creek zone below.

SUMMARY AND CONCLUSIONS

Greater Aneth oil field, Utah's largest oil producer, is a mature, major western U.S. oil field. Located in the Paradox Basin of southeastern Utah, Greater Aneth is a stratigraphic trap, with minor fractures and small faults. The field produces oil and gas from carbonate reservoir rocks in the Desert Creek zone of the Pennsylvanian (Desmoinesian) Paradox Formation. Greater Aneth field is divided into four drilling units. The Aneth Unit is located in the northwestern part of the field. Production in the Aneth Unit had declined by 50% over the past 20 years as the waterflood operations and horizontally drilled wells have matured, but has improved due to a relatively recent CO_2 flood program. The Greater Aneth field has produced over 483 million BO of the estimated 1100 million bbls of OOIP within the field; the Aneth Unit has produced more than 160 million BO of the estimated 386 million barrels of OOIP within the unit (Babcock, 1978a; Utah Division of Oil, Gas and Mining, 2017a). The large amount of remaining oil at Greater Aneth field (and in the Aneth Unit in paricular) made it ideal to demonstrate both EOR by CO_2 flooding and CO_2 storage capacity.

The Gothic shale within the Paradox Formation is the primary seal for the Desert Creek reservoir in Greater Aneth field. Geochemical, petrological, petrophysical, and geomechanical analyses determined the (1) geologic controls on sealing effeciency, (2) effects of pressure changes on seal efficiency due to CO_2 injection and storage, and (3) chemical interaction between CO_2 and the seal at its contact with the reservoir through time. The major findings of these analyses are as follows.

- The Gothic shale is an effective seal above the Desert Creek reservoir, despite micropores and fractures. The Gothic ranges in thickness from 7 to 26 feet (2–8 m), averaging 15 feet (4.6 m) thick. The lateral extent and shape of the underlying Desert Creek carbonate buildup complex is reflected as elevated areas on the structural map of the top of the Gothic. The integrity of the seal is unaffected in areas of thin Gothic shale based on high cumulative oil production from wells there. In addition, much of the overlying lower Ismay and uppermost Desert Creek are non-reservoir rock.

- The core from the Aneth Unit No. H-117 well is an excellent representation of the Gothic shale. The Gothic core is a remarkably uniform mudstone-shale with grain size ranging between clay and silt deposited in low-energy, deep-water offshore marine to shallow, nearshore environments. The quartz silt in some intervals is from a source to the west-southwest. Accessories and biological constituents consist of ubiquitous authigenic pyrite, microfossils, shell fragments, conodonts, and conulariids. The other few cores in the Aneth Unit that include the Gothic show little lateral variability from what was observed in the Aneth Unit No. H-117 core.

- The Gothic may also be a self-sourcing shale-gas or oil-shale reservoir. Total organic carbon ranges from 2.2% to 4.4% with type II kerogen. Hydro-

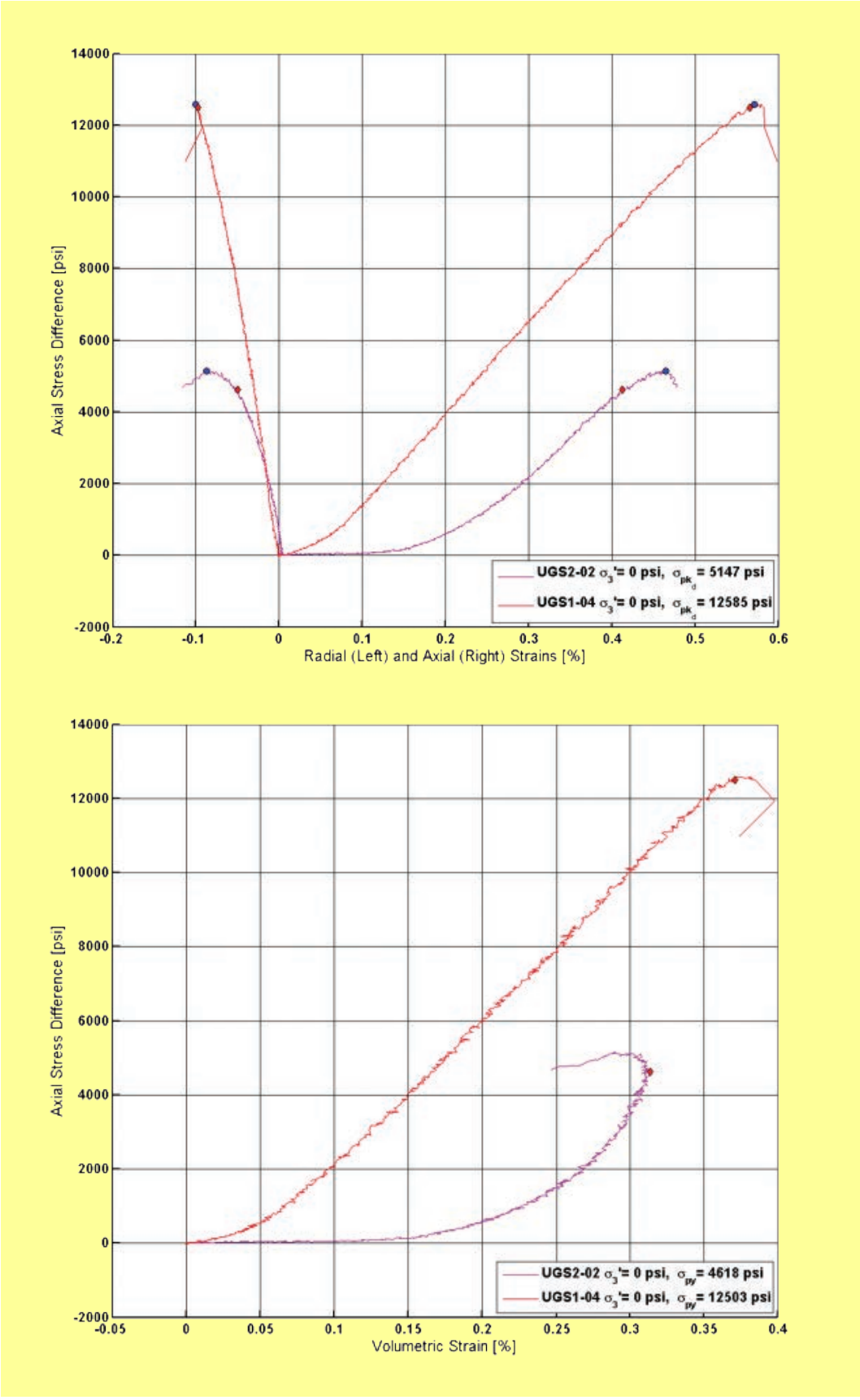

Figure 25. *Results of unconfined compression testing.* ***A.*** *Axial stress difference versus radial and axial strains.* ***B.*** *Axial stress difference versus volumetric strain.*

C

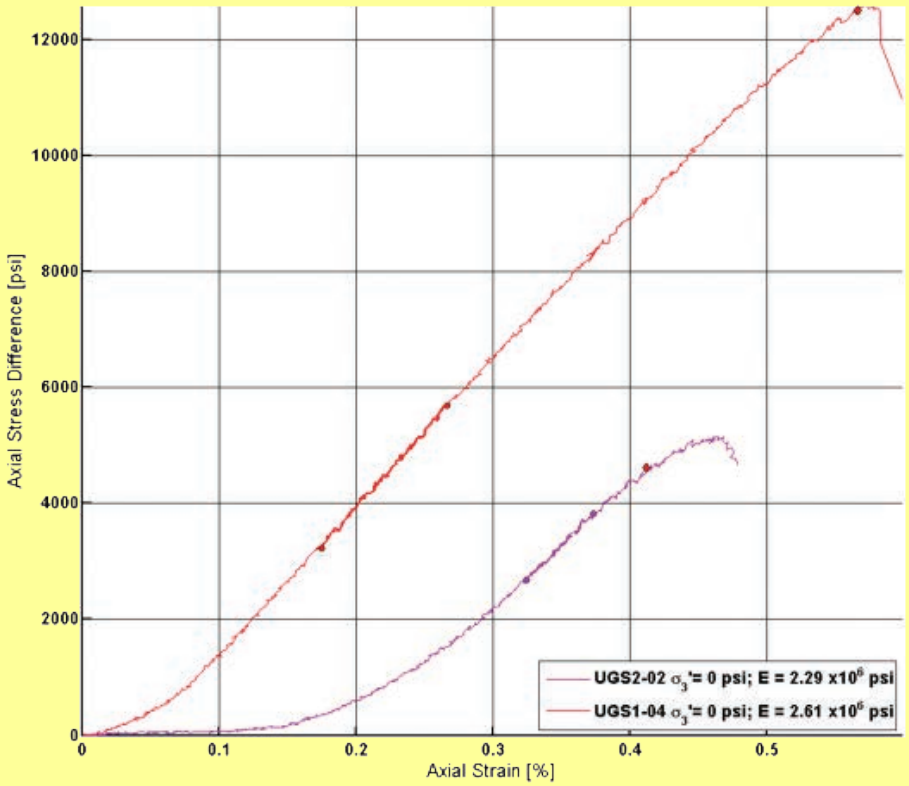

D

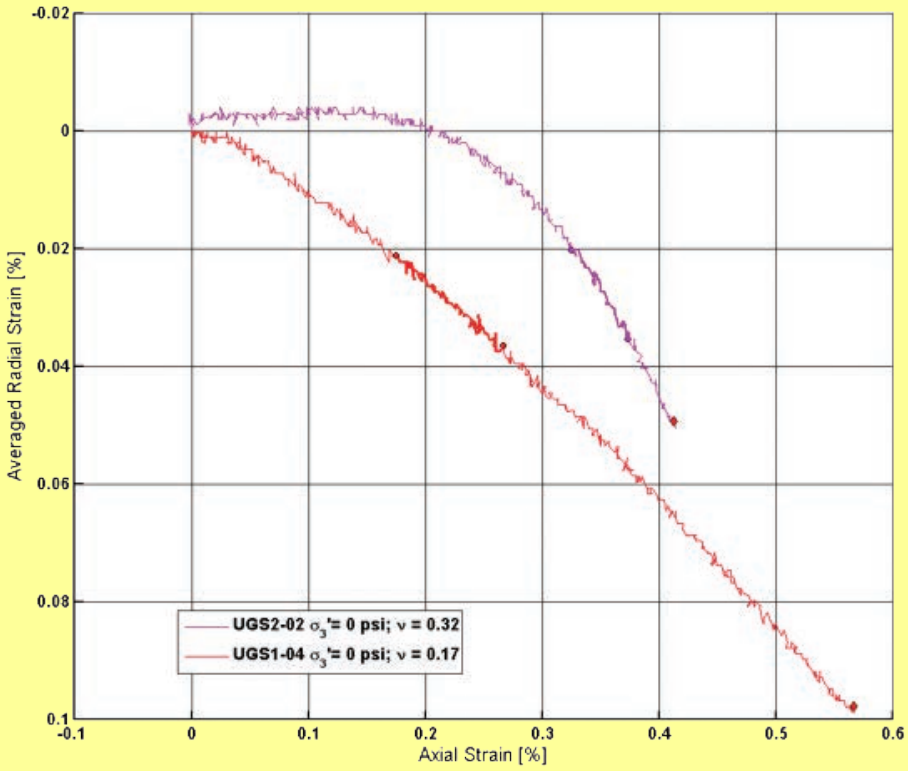

Figure 25 continued. C. *Axial stress difference versus axial strain.* ***D.*** *Averaged radial strain versus axial strain.*

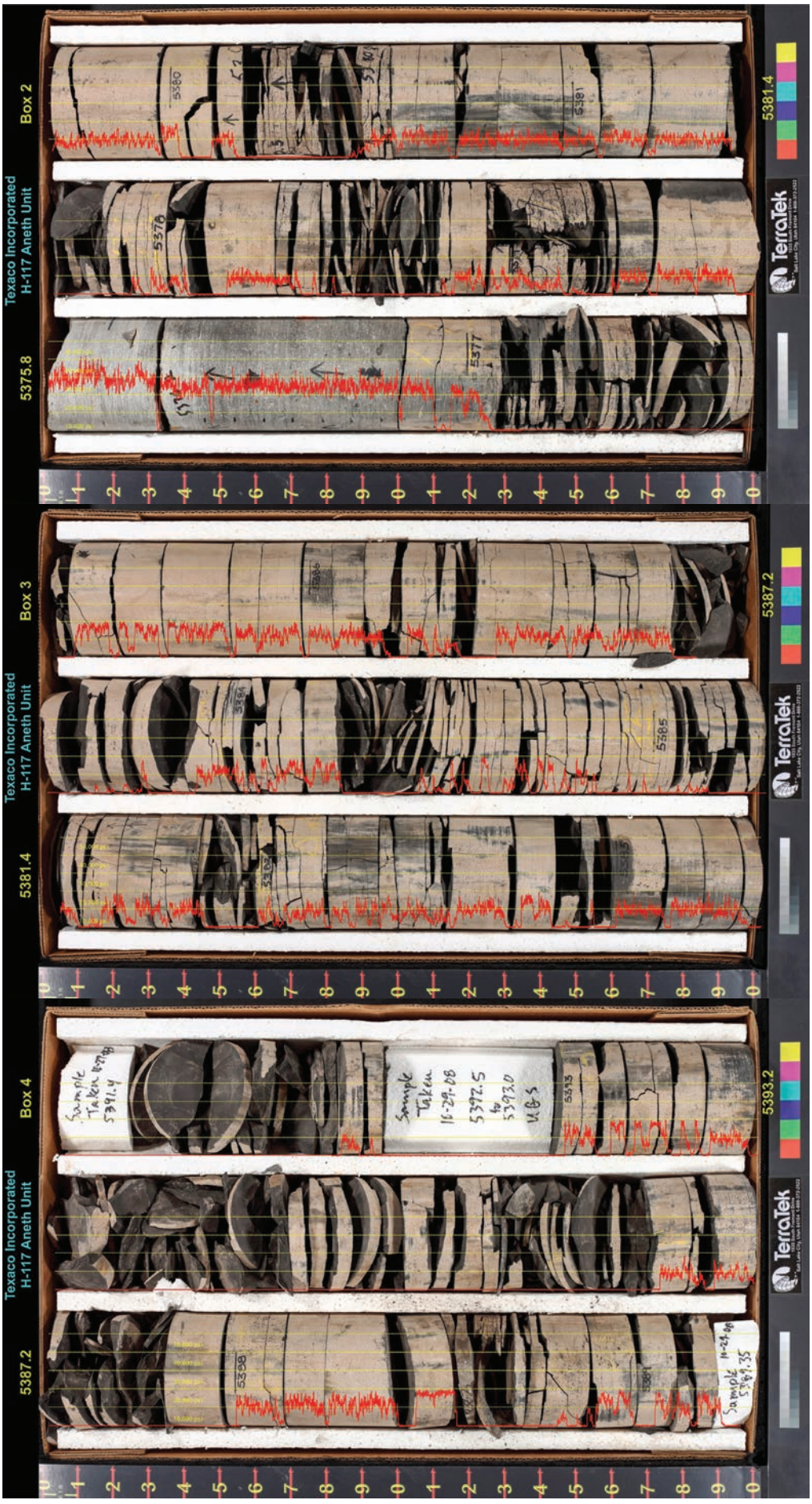

Figure 26. *Continuous unconfined compressive strength profile (red line in psi [no scale provided]) of the Gothic shale core from the Aneth Unit No. H-117 well. Scale bars = 2 feet (showing tenths of a foot increments).*

carbons generated in the Gothic may have also charged adjacent, isolated porous dolomite units in the lower Ismay zone.

- The Gothic consists of four principal lithotypes: argillaceous shale, argillaceous mudstone, silty calcareous-argillaceous mudstone, and phosphatic argillaceous mudstone. Lithology consists of argillaceous or calcareous shale and mudstone composed of a clayey to siliceous matrix with weak laminations defined by micas. Within the matrix, calcite crystals, pyrite, quartz, microfossils, flakes of organics, and swarms of intercrystalline micropores are common. Argillaceous shale and mudstone, representing the deeper water, offshore marine environments are the best seals whereas the minor shallow, nearshore silt-rich mudstone will be more brittle. However, Young's modulus and Poisson's ratio analyses suggest that the Gothic shale overall in the Aneth Unit is not brittle.

- Inclined and horizontal shear fractures or fracture zones are found in the Gothic shale. Near the base of the Gothic section, vertical to subvertical extensional fractures are present. Mineralization within these natural fractures is most likely dominated by carbonates and organics. Fractures that could connect Desert Creek reservoir rock through the Gothic shale into the Ismay zone are a low potential concern for hydrocarbon and CO_2 leakage.

- Porosity ranges from 2.7% to 3.4% and pressure-decay permeability is no greater than 0.000146 mD. These and other basic matrix petrophysical parameters indicate the Gothic shale to be a highly effective reservoir seal.

- The Gothic shale should support very large CO_2 or hydrocarbon columns based on mercury injection capillary pressure and pore aperture distribution analyses.

- Continuous unconfined compressive strength profiles show a relatively uniform homogenous shale package. Compressional testing suggests some degree of hydraulic fracture containment.

We conclude that the Gothic shale within the Aneth Unit, as well as the entire Greater Aneth field, has provided the seal for the hydrocarbons stored in the Desert Creek zone for millions of years. More significantly, our data show that the Gothic is capable of effectively sealing large amounts of CO_2 injected into the Desert Creek currently for use in EOR or in the future as geological storage of anthropogenic CO_2 produced from coal-fired power plant point sources on the Colorado Plateau.

ACKNOWLEDGMENTS

This research was performed under the direction of the New Mexico Institute of Mining and Technology, Brian McPherson, Project Manager and Principal Investigator, as part of the Southwest Regional Partnership on Carbon Sequestration—Phase II: Field Demonstrations Project. This project was funded by the U.S. Department of Energy through the National Energy Technology Laboratory, Contract No. DE-FC26-05NT42591. Support was also provided by the Utah Geological Survey (UGS). Sandia is a multi-mission laboratory operated by Sandia Corporation, a wholly owned subsidiary of Lockheed Martin Company, for the U.S. Department of Energy's National Nuclear Security Administration under contract DE-ACOC4-94AL85000.

James Parker (deceased) and Cheryl Gustin of the UGS and Susan Heath (of New Mexico Tech at the time) prepared some figures; Michael Laine (retired), Ammon McDonald (now with the Utah Division of Oil, Gas and Mining), and Thomas Dempster of the UGS assisted with sample preparation and core photography. Geochemical, petrophysical, petrographic, and geomechanical analyses were conducted by TerraTek – A Schlumberger Company, Salt Lake City, Utah; Sandia National Laboratories, Albuquerque, New Mexico; and Poro-Technology, Houston, Texas.

This study was carefully reviewed by David Tabet (retired), Craig Morgan, and Kimm Harty (retired) of the UGS; and Samuel M. Hudson of the Department of Geological Sciences, Brigham Young University. Their suggestions and constructive criticism greatly improved the manuscript. Finally, we thank Vicky Clarke, Jen Miller, and the UGS editorial production team for their efforts in producing this publication.

REFERENCES

Amateis, L.J., 1995, Application of sequence stratigraphic modeling to integrated reservoir management at Aneth Unit, Greater Aneth field, Utah: Society of Petroleum Engineers, SPE Paper 030534, p. 35–49.

Andreani, M., Gouze, P., Luquot, L., and Jouanna, P., 2008, Changes in seal capacity of fractured claystone caprocks induced by dissolved and gaseous CO_2 seepage: Geophysical Research Letters, v. 35, p. 6.

Aplin, A.C., and Larter, S.R., 2005, Fluid flow, pore pressure, wetability, and leakage in mudstone cap rocks, *in* Boult, P., and Kaldi, J., editors, Evaluating fault and cap rock seals: American Association of Petroleum Geologists Hedberg Series, no. 2, p. 1–12.

Babcock, P.A., 1978a, Aneth (Aneth Unit), San Juan County, Utah, *in* Fassett, J.E., editor, Oil and gas fields in the Four Corners area: Four Corners Geological Society Guidebook, v. II, p. 577–579.

Babcock, P.A., 1978b, Aneth (McElmo Creek Unit), San Juan County, Utah, *in* Fassett, J.E., editor, Oil and gas fields in the Four Corners area: Four Corners Geological Society Guidebook, v. II, p. 580–583.

Babcock, P.A., 1978c, Aneth (Ratherford Unit), San Juan County, Utah, *in* Fassett, J.E., editor, Oil and gas fields in the Four Corners area: Four Corners Geological Society Guidebook, v. II, p. 584–586.

Babcock, P.A., 1978d, Aneth (White Mesa Unit), San Juan County, Utah, *in* Fassett, J.E., editor, Oil and gas fields in the Four Corners area: Four Corners Geological Society Guidebook, v. II, p. 587–590.

Bereskin, S.R., and McLennan, J., 2008, Hydrocarbon potential of Pennsylvanian black shale reservoirs, Paradox Basin, southeastern Utah: Utah Geological Survey Open-File Report 534, 53 p.

Bereskin, S.R., and McLennan, J.D., 2009, Gas shale reservoir characteristics from the Pennsylvanian of southeastern Utah, USA [abs.]: American Association of Petroleum Geologists, Convention Abstracts, v. 18, p. 20.

Bereskin, S.R., Chidsey, T.C., Jr., and McLennan, J.D., 2010, Pennsylvanian organic mudstone reservoir characteristics from the Paradox Basin, southeastern Utah [abs.]: American Association of Petroleum Geologists, Rocky Mountain Section Meeting Program with Abstracts, p. 40.

Chidsey, T.C., Jr., editor, 2016, Paleozoic shale-gas resources of the Colorado Plateau and eastern Great Basin, Utah—multiple frontier exploration opportunities: Utah Geological Survey Bulletin 136, 241 p., 21 appendices.

Chidsey, T.C., Jr., and Eby, D.E., 2014, Reservoir properties and carbonate petrography of the Aneth Unit, Greater Aneth field, Paradox Basin, southeastern Utah, *in* MacLean, J.S., Biek, R.F., and Huntoon, J.E., editors, Geology of Utah's far south: Utah Geological Association Publication 43, p. 153–197, 2 appendices, 6 plates.

Chidsey, T.C., Jr., Eby, D.E., and Lorenz, D.M., 1996, Geological and reservoir characterization of small shallow-shelf fields, southern Paradox Basin, Utah, *in* Huffman, A.C., Jr., Lund, W.R., and Godwin, L.H., editors, Geology and resources of the Paradox Basin: Utah Geological Association Publication 25, p. 39–56.

Couples, G.D., 2005, Seals—the role of geomechanics rocks, *in* Boult, P., and Kaldi, J., editors, Evaluating fault and cap rock seals: American Association of Petroleum Geologists Hedberg Series, no. 2, p. 87–108.

De Winter, D.A.M., Schneijdenberg, C., Lebbink, M.N., Lich, B., Verkleij, A.J., Drury, M.R., and Humbel, B.M., 2009, Tomography of insulating biological and geological materials using focused ion beam (FIB) sectioning and low-kV BSE imaging: Journal of Microscopy, v. 233, p. 372–383.

Fredrich, J.T., 1999, 3D imaging of porous media using laser scanning confocal microscopy with application to microscale transport processes: Elsevier, Physics and Chemistry of the Earth, Part A—Solid Earth and Geodesy, v. 24, issue 7, p. 551–561.

Harr, C.L., 1996, Paradox oil and gas potential of the Ute Mountain Ute Indian Reservation, *in* Huffman, A.C., Jr., Lund, W.R., and Godwin, L.H., editors, Geology of the Paradox Basin: Utah Geological Association Publication 25, p. 13–28.

Heath, J.E., Dewers, T.A., McPherson, B.J.O.L., Petrusak, R., Chidsey, T.C., Jr., Rinehart, A.J., and Mozley, P.S., 2011, Pore networks in marine and non-marine mudstones—characteristics and controls on sealing behavior, *in* Advances in 3D imaging and analysis of geomaterials: Geosphere, v. 7, no. 2, p. 429–454.

Hite, R.J., 1960, Stratigraphy of the saline facies of the Paradox Member of the Hermosa Formation of southeastern Utah and southwestern Colorado, *in* Smith, K.G., editor, Geology of the Paradox Basin fold and fault belt: Four Corners Geological Society, Third Field Conference Guidebook, p. 86–89.

Hite, R.J., and Cater, F.W., 1972, Pennsylvanian rocks and salt anticlines, Paradox Basin, Utah and Colorado, *in* Mallory, W.W., editor, Geologic atlas of the Rocky Mountain region: Rocky Mountain Association of Geologists Guidebook, p. 133–138.

Kitcho, C.H., 1981, Characteristics of surface faults in the Paradox Basin, *in* Wiegand, D.L., editor, Geology of the Paradox Basin: Rocky Mountain Association of Geologists Guidebook, p. 1–21.

Lindeberg, E., 2002, The quality of a CO_2 repository—What is the sufficient retention time of CO_2 stored underground?, *in* Gale, J., and Kaya, Y., editors, Proceedings of 6th Greenhouse Gas Control Technologies Conference: Kyoto, Japan, Elsevier, p. 255–260.

Lu, J., Wilkinson, M., Haszeldine, R.S., and Fallick, A.E., 2009, Long-term performance of a mudrock seal in natural CO_2 storage: Geology, v. 37, no. 1, p. 35–38.

Moore, T.R., and Hawks, R.L., 1993, Greater Aneth, *in* Hill, B.G., and Bereskin, S.R., editors, Oil and gas fields of Utah: Utah Geological Association Publication 22 (Addendum), non-paginated.

Moreland, P.G., and Wray, L., 2009, The Pennsylvanian Gothic shale gas resource play of the Paradox Basin [abs.]: American Association of Petroleum Geologists, Convention Abstracts, v. 18, p. 147.

Morgan, C.D., Carney, S., Chidsey, T.C., Jr., Sprinkel, D.A., Herbst, S., Waanders, G., Eby, D.E., Schamel, S., and Gianniny, G.L., 2016, Chapter 8—regional correlations and outcrop analogs, *in* Chidsey, T.C., Jr., editor, Paleozoic shale-gas resources of the Colorado Plateau and eastern Great Basin, Utah—multiple frontier exploration opportunities: Utah Geological Survey Bulletin 136, p. 145–171.

Peterson, J.A., 1992, Aneth field—U.S.A., Paradox Basin, Utah, *in* Foster, N.H., and Beaumont, E.A., editors, Strati-

graphic traps III: American Association of Petroleum Geologists Treatise of Petroleum Geology—Atlas of Oil and Gas Fields, p. 41–82.

Peterson, J.A., and Ohlen, H.R., 1963, Pennsylvanian shelf carbonates, Paradox Basin, *in* Bass, R.O., editor, Shelf carbonates of the Paradox Basin: Four Corners Geological Society Symposium, Fourth Field Conference, p. 65–79.

Reid, F.S., and Berghorn, C.E., 1981, Facies recognition and hydrocarbon potential of the Pennsylvanian Paradox Formation, *in* Wiegand, D.L., editor, Geology of the Paradox Basin: Rocky Mountain Association of Geologists Guidebook, p. 111–117.

Schamel, S., 2005, Shale gas reservoirs of Utah—survey of an unexploited potential energy resource: Utah Geological Survey Open-File Report 461, 114 p.

Schamel, S., 2006, Shale gas resources of Utah—assessment of previously undeveloped gas discoveries: Utah Geological Survey Open-File Report 499, 85 p.

Stowe, C., 1972, Oil and gas production in Utah to 1970: Utah Geological and Mineral Survey Bulletin 94, p. 170.

Utah Division of Oil, Gas and Mining, 2017a, Oil and gas summary production report by field, December 2016: Online, http://oilgas.ogm.utah.gov/pub/Publications/Reports/Prod/Field/Fld_Dec_2016.pdf, accessed April 2017.

Utah Division of Oil, Gas and Mining, 2017b, Oil and gas summary production report by well, December 2016: Online, http://oilgas.ogm.utah.gov/pub/Publications/Reports/Prod/Well/Wel_Dec_2016.pdf, accessed April 2017.